

Overexpression of Arabidopsis ECERIFERUM1 promotes wax very-long-chain alkane biosynthesis and influences plant response to biotic and abiotic stresses

Brice Bourdenx, Amelie Bernard, Frederic Domergue, Stéphanie Pascal, Amandine Leger, Dominique Roby, Marjorie Pervent, Denis Vile, Richard P. Haslam, Johnathan A. Napier, et al.

▶ **To cite this version:**

Brice Bourdenx, Amelie Bernard, Frederic Domergue, Stéphanie Pascal, Amandine Leger, et al.. Overexpression of Arabidopsis ECERIFERUM1 promotes wax very-long-chain alkane biosynthesis and influences plant response to biotic and abiotic stresses. Plant Physiology, 2011, 156 (1), pp.29-45. 10.1104/pp.111.172320 . hal-02651224

HAL Id: hal-02651224
https://hal.inrae.fr/hal-02651224

Submitted on 29 May 2020

HAL is a multi-disciplinary open access archive for the deposit and dissemination of scientific research documents, whether they are published or not. The documents may come from teaching and research institutions in France or abroad, or from public or private research centers.

L'archive ouverte pluridisciplinaire **HAL**, est destinée au dépôt et à la diffusion de documents scientifiques de niveau recherche, publiés ou non, émanant des établissements d'enseignement et de recherche français ou étrangers, des laboratoires publics ou privés.

Overexpression of Arabidopsis *ECERIFERUM1* Promotes Wax Very-Long-Chain Alkane Biosynthesis and Influences Plant Response to Biotic and Abiotic Stresses[1][W]

Brice Bourdenx, Amélie Bernard, Frédéric Domergue, Stéphanie Pascal, Amandine Léger, Dominique Roby, Marjorie Pervent, Denis Vile, Richard P. Haslam, Johnathan A. Napier, René Lessire, and Jérôme Joubès*

Laboratoire de Biogenèse Membranaire, Unité Mixte de Recherche 5200, Centre National de la Recherche Scientifique-Université Bordeaux Segalen, 33076 Bordeaux cedex, France (B.B., A.B., F.D., S.P., R.L., J.J.); Laboratoire des Interactions Plantes-Microorganismes, Unité Mixte de Recherche Centre National de la Recherche Scientifique-Institut National de la Recherche Agronomique 2594/441, 31326 Castanet-Tolosan cedex, France (A.L., D.R.); Laboratoire d'Ecophysiologie des Plantes sous Stress Environnementaux, Unité Mixte de Recherche 759, Institut National de la Recherche Agronomique-SupAgro, 34060 Montpellier cedex, France (M.P., D.V.); and Rothamsted Research, Harpenden, Hertshire AL5 2JQ, United Kingdom (R.P.H., J.A.N.)

Land plant aerial organs are covered by a hydrophobic layer called the cuticle that serves as a waterproof barrier protecting plants against desiccation, ultraviolet radiation, and pathogens. Cuticle consists of a cutin matrix as well as cuticular waxes in which very-long-chain (VLC) alkanes are the major components, representing up to 70% of the total wax content in Arabidopsis (*Arabidopsis thaliana*) leaves. However, despite its major involvement in cuticle formation, the alkane-forming pathway is still largely unknown. To address this deficiency, we report here the characterization of the Arabidopsis *ECERIFERUM1* (*CER1*) gene predicted to encode an enzyme involved in alkane biosynthesis. Analysis of *CER1* expression showed that *CER1* is specifically expressed in the epidermis of aerial organs and coexpressed with other genes of the alkane-forming pathway. Modification of *CER1* expression in transgenic plants specifically affects VLC alkane biosynthesis: waxes of TDNA insertional mutant alleles are devoid of VLC alkanes and derivatives, whereas *CER1* overexpression dramatically increases the production of the odd-carbon-numbered alkanes together with a substantial accumulation of iso-branched alkanes. We also showed that *CER1* expression is induced by osmotic stresses and regulated by abscisic acid. Furthermore, *CER1*-overexpressing plants showed reduced cuticle permeability together with reduced soil water deficit susceptibility. However, *CER1* overexpression increased susceptibility to bacterial and fungal pathogens. Taken together, these results demonstrate that *CER1* controls alkane biosynthesis and is highly linked to responses to biotic and abiotic stresses.

Terrestrial plants have developed a barrier preventing uncontrolled water loss, the cuticle, which controls water movements between the outer cell wall of the epidermis and the surrounding atmosphere adjacent to the plant. The cuticle is a rather thin membrane consisting of cutin, which is the main structural component of the cuticular matrix, and associated solvent-soluble lipids called cuticular waxes. Cutin is a three-dimensional polymer of mostly C16 and C18 hydroxy fatty acids cross-linked by ester bonds (Pollard et al., 2008; Li and Beisson, 2009), whereas cuticular wax is a complex mixture of a homolog series of very-long-chain (VLC) aliphatic lipids, triterpenoids, and minor secondary metabolites, such as sterols and flavonoids (Kunst and Samuels, 2009). The physical and chemical properties of cuticular waxes determine vital functions for plants. Indeed, besides playing a major role in protecting the plant aerial parts from uncontrolled water loss (Shepherd and Wynne Griffiths, 2006; Kosma et al., 2009), waxes protect plants against UV radiation and help to minimize deposits of dust, pollen, and air pollutants (Kunst and Samuels, 2003). In addition, surface wax is believed to play important roles in plant defense against bacterial and fungal pathogens (Riederer, 2006) and has been shown to participate in a variety of plant-insect interactions (Eigenbrode et al., 2000).

[1] This work was supported by the Ministère de l'Enseignement Supérieur et de la Recherche (doctoral fellowships for B.B., A.B., and A.L.), by the Centre National de la Recherche Scientifique and the University Bordeaux Segalen, and by the Biotechnology and Biological Sciences Research Council (grant support to Rothamsted Research).

* Corresponding author; e-mail jjoubes@biomemb.u-bordeaux2.fr.

The author responsible for distribution of materials integral to the findings presented in this article in accordance with the policy described in the Instructions for Authors (www.plantphysiol.org) is: Jérôme Joubès (jjoubes@biomemb.u-bordeaux2.fr).

[W] The online version of this article contains Web-only data.
www.plantphysiol.org/cgi/doi/10.1104/pp.111.172320

The wax aliphatic compounds originate from the very-long-chain fatty acids (VLCFAs), with predominant chain lengths ranging from 26 to 32 carbons, which result from the acyl-CoA elongase activity in the plant epidermal cells (Zheng et al., 2005; Bach et al., 2008; Joubès et al., 2008; Beaudoin et al., 2009). The wax components are then produced according to two different pathways: (1) the alcohol-forming pathway, which produces VLC primary alcohols and wax esters; and (2) the alkane-forming pathway leading to the formation of VLC alkanes and their derivatives, which account for 70% to 80% of total wax in Arabidopsis (*Arabidopsis thaliana*; Jetter and Kunst, 2008). In leaves, the alkane-forming pathway mainly leads to the formation of VLC alkanes, which represent more than 70% of total wax components. In stems, VLC alkanes account for only 50% of total waxes, but since secondary alcohols and ketones, which represent more than 30% of total wax components, derive directly from VLC alkanes, the alkane-forming pathway is responsible for more than 80% of the total stem wax.

Several Arabidopsis *eceriferum* (*cer*; literally "not carrying wax") mutants affected in wax biosynthesis and more precisely in alkane biosynthesis have been easily identified on the basis of increased stem glossiness (Koornneef et al., 1989; Hannoufa et al., 1993; McNevin et al., 1993; Jenks et al., 1995). The wax composition analysis of this set of mutants led to a hypothetical alkane-forming pathway: VLCFAs would be reduced to intermediate aldehydes from which alkanes could be formed by decarbonylation; hydroxylation of alkanes would then result in secondary alcohol formation, and oxidation of these alcohols would lead to the corresponding ketones. Nevertheless, when the genes identified in these mutants were cloned, they did not provide enough clues to define the biochemical function of the corresponding proteins (Samuels et al., 2008). This is in contrast to the alcohol-forming pathway, for which genes have been clearly identified and the corresponding proteins functionally characterized (Rowland et al., 2006; Li et al., 2008). Indeed, the alkane-forming pathway remains largely unknown: *CER3* could be the fatty acid reductase responsible for aldehyde formation (Chen et al., 2003), *CER1* would then encode the alkane-forming enzyme (Aarts et al., 1995), while *MAH1* most probably would encode the mild-chain alkane hydroxylase (Greer et al., 2007). However, no biochemical activity has been associated with any of these proteins, and their hypothetical role in the alkane-forming pathway only relies on defects in wax composition.

Arabidopsis *cer3* (*cer3/wax2/yre/flp1*) showed an alteration in the cuticle membrane and cuticular waxes. In addition, the mutation had some pleiotropic effects, typical of cutin-defective mutants, including postgenital organ fusions, conditional male sterility, decrease of the stomatal index, and trichome development (Ariizumi et al., 2003; Chen et al., 2003; Kurata et al., 2003). Nevertheless, the mutation did not affect the cutin load and composition (Rowland et al., 2007). Alteration of the waxes was associated with increased stem glossiness, and the quantitative analysis of epicuticular waxes showed a decrease of 78% of the total wax load in the stem of the mutant. Modification of the wax load was due to a decrease of all the compounds of the alkane-forming pathway together with an increase of the alcohol-forming pathway-derived compounds, notably the amount of C30 primary alcohols (Chen et al., 2003). Based on this phenotype, *CER3* could encode an aldehyde-generating enzyme responsible for the VLCFA reduction to intermediate aldehydes (Kurata et al., 2003).

Recently, an enzyme involved in alkane hydroxylation to secondary alcohols and possibly ketones has been identified as the cytochrome P450 CYP96A15 called MAH1 (Suh et al., 2005; Greer et al., 2007). Analysis of insertional mutants showed an absence of secondary alcohols and ketones in stem wax together with an increase of the alkane content, compensating for the loss of alkane derivatives. Interestingly, the ectopic expression of the gene under the control of the cauliflower mosaic virus 35S promoter led to the production of secondary alcohols and ketones in leaves, in which they are normally not produced, supporting the hypothesis that MAH1 catalyzes the alkane hydroxylation to secondary alcohols.

The Arabidopsis *cer1* stem wax composition was characterized by a dramatic decrease in products of the alkane-forming pathway (e.g. alkanes, secondary alcohols, and ketones), with the exception of aldehydes, in which the amount was slightly increased (Hannoufa et al., 1993; McNevin et al., 1993; Jenks et al., 1995). Analysis of the CER1 protein primary structure revealed the presence of several transmembrane domains, a metal ion-binding domain, and a fatty acid hydroxylase conserved domain (Aarts et al., 1995). Based on these observations, *CER1* was proposed to encode the aldehyde decarbonylase, catalyzing the alkane biosynthesis. More recently, the CER1 subcellular localization, together with CER3 and MAH1, in the endoplasmic reticulum membranes (Greer et al., 2007; Kamigaki et al., 2009) supported the idea that CER1 could be involved in the alkane-forming pathway. Nevertheless, while CER1 could be involved in a major step of wax production, almost no molecular data concerning *CER1* have been reported so far.

In this paper, results that further improve our understanding of the *CER1* gene in Arabidopsis are presented. The expression of *CER1*, along with other genes of the alkane-forming pathway, was analyzed in detail in the different organs of Arabidopsis and under different stress conditions. Using several *CER1*-overexpressing lines and TDNA insertional mutants, we characterized the effects of a deregulation of *CER1* expression on cuticular wax content and, more particularly, on VLC alkane biosynthesis. Finally, the effects of the modification of VLC alkane production on plant growth and development, cuticle properties, as well as plant responses to soil water deficit and pathogen attack were analyzed.

RESULTS

Expression Profiling of the Genes Involved in the Alkane-Forming Pathway in Arabidopsis Organs

A search for *CER1-like* genes in Arabidopsis databases (http://www.arabidopsis.org/) allowed the identification of a total of four different genes encoding CER1-like proteins: *CER1*, At1g02205; *CER1-like1*, At1g02190; *CER1-like2*, At2g37700; and *CER1-like3*, At5g28280. These four genes form a small gene family in which two are highly homologous to *CER1*, *CER1-like1* and *CER1-like2*, whereas *CER1-like3* appears as a pseudogene in The Arabidopsis Information Resource database. The organ distribution of *CER1* and the three *CER1-like* genes was determined by real-time PCR (Fig. 1A). The expression of *CER3* and *MAH1*, potentially involved in the alkane-forming pathway, was also analyzed. *CER1* was expressed in seedlings, stems, leaves, flowers, and siliques. We did not detect transcripts in roots. Among the three *CER1-like* genes, only *CER1-like1* was found expressed in reproductive organs. The *CER1-like2* and *CER1-like3* transcripts were never detected in any tissues or conditions. This result is in agreement with microarray data available in the Genevestigator gene expression database (http://www.genevestigator.ethz.ch/). Furthermore, these data indicate that *CER1* and *CER1-like1* are expressed in all flower tissues, except pollen for both genes and pedicel for *CER1-like1*, and in pods but not in seeds. *CER3*, which showed an expression pattern similar to that of *CER1*, is highly expressed in vegetative and reproductive organs compared with the very low expression in roots. Microarray data indicated similar results and showed that *CER3* is expressed in all flower tissues, except pollen, and in seeds. Concerning *MAH1*, we found a pattern of expression in accordance with its putative alkane hydroxylase activity. Indeed, *MAH1* was not expressed in roots or vegetative organs, except in stems. It was also expressed in flowers and siliques. Genevestigator data indicated that *MAH1* is only expressed in the carpel and the pedicel of flowers and in pods but not in seeds. Interestingly, the three genes *CER1*, *CER3*, and *MAH1* appeared coexpressed in almost all tissues that we have examined, supporting their putative role in the same pathway. Moreover, this set of data suggested that of the four *CER1-like* genes, only *CER1* expression is correlated with wax biosynthesis in vegetative organs.

To investigate the cell type expression pattern of the *CER1* gene, we generated transgenic Arabidopsis lines expressing the *GUS* reporter gene under the control of the *CER1* promoter (Fig. 1B). In 5-d-old germinating seedlings, expression was detected in the cotyledons, the shoot apical meristem, and the leaf primordia (data not shown). No GUS activity was detected in the hypocotyl and the vascular tissues. In 10-d-old seedlings, *GUS* expression was detected in young rosette leaves (Fig. 1Ba). In 3-week-old plant leaves, expression was preferentially associated with young leaves rather than with mature leaves (Fig. 1Bd), suggesting that *CER1* gene expression is under developmental control.

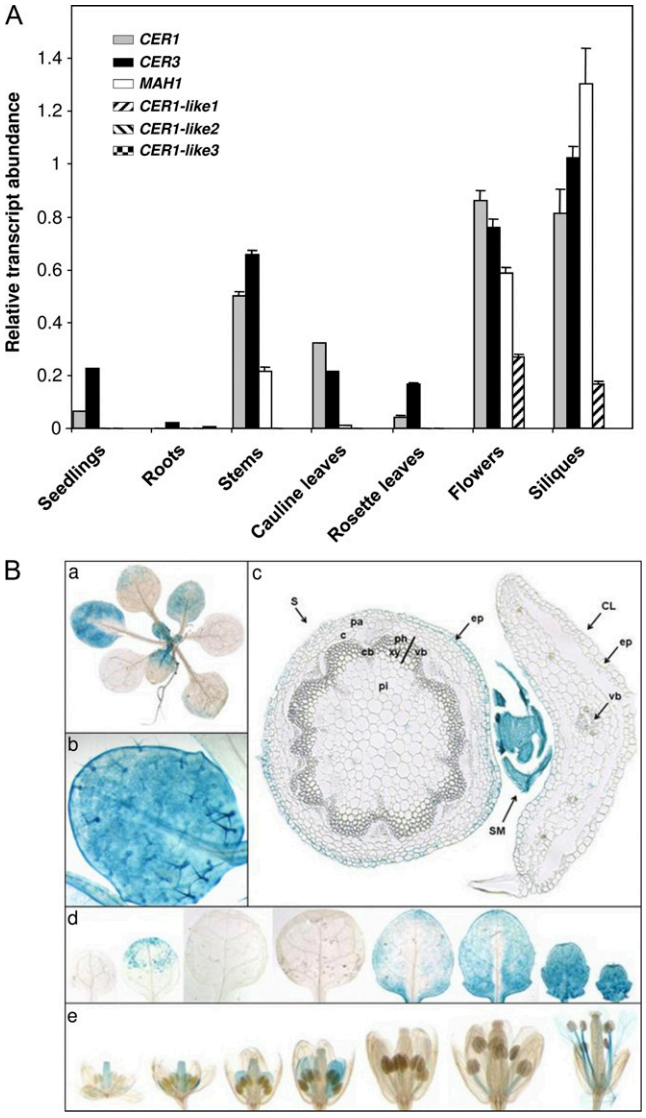


Figure 1. Expression analysis of the *CER1* gene family in Arabidopsis. A, Differential expression analysis of Arabidopsis *CER1-like*, *CER3*, and *MAH1* genes in various organs of Arabidopsis. The gene expression level was determined by real-time RT-PCR analysis. Results are presented as relative transcript abundance. The relative transcript abundance of *ACT2*, *EF-1α*, *eIF-4A-1*, *UBQ10*, and *PP2A* in each sample was determined and used to normalize for differences of total RNA amount. The data represent means ± SD of five replicates. Total RNA was isolated from 15-d-old seedlings, roots, stems, cauline leaves, rosette leaves, flowers, and siliques. B, Spatial expression patterns of the *CER1* gene in transgenic Arabidopsis plants harboring the *CER1* promoter fused to the *GUS* gene. Promoter activity was visualized through histochemical GUS staining on 10-d-old seedlings (a), young leaf of a 3-week-old plant (b), transverse section of the stem (S), secondary meristem (SM), and cauline leaf (CL; c), leaves of a 3-week-old plants (d), and flowers (e). C, Cortex; cb, cambium; ep, epidermis; pa, parenchyma; ph, phloem; pi, pith; vb, vascular bundle; xy, xylem.

Magnification of a young rosette leaf showed strong *GUS* expression in specialized epidermal cell trichomes (Fig. 1Bb). *GUS* expression was analyzed in elongated floral stems of 6-week-old plants, and a cross-section of the stem showed epidermis-specific *GUS* expression (Fig. 1Bc). No GUS activity can be detected in other tissues of the stem. Expression was also specifically localized in the epidermis of cauline leaves (Fig. 1Bc). In young flowers, *CER1* promoter activity was detected in the carpel and the sepals (Fig. 1Be). As the flower matured, *CER1* promoter activity decreased in these tissues and appeared in the stamen filaments and the petals (Fig. 1Be). Cross-sections of flowers showed that *GUS* expression was localized in the epidermis cells of the stamen filaments (data not shown). These results demonstrated that the epidermis-specific *CER1* expression is regulated at the tissue and organ levels throughout plant development, in accordance with its role in wax biosynthesis.

Molecular and Phenotypic Characterization of *CER1*-Overexpressing and TDNA Insertion Arabidopsis Lines

To understand the role of CER1 in cuticular wax production, we generated transgenic Arabidopsis lines that constitutively overexpressed the *CER1* gene under the control of the cauliflower mosaic virus 35S promoter. Among the obtained lines, two lines, *CER1-ox1* and *CER1ox2*, were selected for further analysis. Since previously reported *cer1* mutants were in the genetic background Landsberg *erecta* (Koornneef et al., 1989; Aarts et al., 1995) or Wassilewskija (McNevin et al., 1993), we selected new TDNA insertion mutants in the Arabidopsis ecotype Columbia (Col-0) for comparison with the *CER1*-overexpressing lines. Among the SALK lines identified (http://signal.salk.edu/), two mutant alleles of *CER1*, *cer1-1* (SALK_008544) and *cer1-2* (SALK_014839), were selected and analyzed (Fig. 2A). The TDNA insertion in *cer1-1* disrupted the last exon of the *CER1* gene (at nucleotide 3,191 relative to the start codon), while in *cer1-2*, the *CER1* gene was disrupted in the 5′-untranslated region (at nucleotide 266 before the start codon). In addition, the *cer1-1* allele was complemented with a construct harboring the *CER1* gene under the control of *Pro-35S* and, among obtained lines, one line was selected for further analysis (*cer1-1R*). TDNA insertions were confirmed by PCR on genomic DNA (Fig. 2B).

CER1 gene expression was analyzed in all transgenic lines by semiquantitative reverse transcription (RT)-PCR (Fig. 2C). No full-length transcripts were detected in the *cer1-1* allele. Although full-length transcripts could be detected in the *cer1-2* allele, the transcript level was greatly reduced compared with wild-type plants. The *cer1-1* rescued line and both overexpressing lines exhibited a higher level of transcripts as compared with wild-type plants. This observation was confirmed by RT-quantitative PCR analysis showing a 40-fold increase of the transcripts in the *cer1-1* rescued line and a more than 80-fold increase in both overexpressing lines as compared with wild-type plants (Fig. 2D).

The effect of changes in *CER1* transcript levels in the different lines can be easily visualized by modification of the stem's optical properties (Fig. 2E). Indeed, compared with wild-type plants, *cer1-1* and *cer1-2* lines exhibited a bright green stem phenotype due to qualitative and/or quantitative changes of stem cuticular wax production, which is characteristic of wax-deficient mutants. *CER1* overexpression in the *cer1-1* allele prevents this glossy phenotype, confirming that it is linked to *CER1* inactivation. The *CER1* overexpression in the wild-type background did not modify the stem brightness. These observations were confirmed by scanning electron microscopy analysis of young stem surfaces of wild-type, *cer1-1*, *cer1-1R*, and *CER1ox1* lines (Fig. 2F). The *CER1* inactivation in *cer1-1* led to a complete disappearance of the wax crystals formed on the stem surface. *CER1* overexpression in the *cer1-1* background rescued wax crystal formation, whereas *CER1* overexpression in the wild-type background did not modify their formation.

Modification of *CER1* Expression Disturbs Wax Production at the Surface of the Plant Aerial Organs

In order to assess the effect of deregulating *CER1* expression on wax biosynthesis, cuticular wax composition of stems and leaves of the different lines, Col-0 (wild type), *cer1-1*, *cer1-2*, *cer1-1R*, *CER1ox1*, and *CER1ox2*, was analyzed in detail (Tables I and II; Fig. 3; Supplemental Figs. S1 and S2). The wax load per unit of stem area of the *cer1-1* and *cer1-2* alleles was strongly reduced compared with wild-type plants (84% and 70% decreases, respectively). The *cer1-1* allele was more affected than the *cer1-2* allele, probably due to the residual *CER1* expression in the *cer1-2* mutant (Fig. 2). In both alleles, this decrease was largely due to a reduced amount of the three major components of the stem wax produced by the alkane-forming pathway, which accounts for 68% of the total stem wax load in wild-type plants: the C29 alkane (99.6% and 81% decreases, respectively), the C29 secondary alcohol (99.4% and 95% decreases, respectively), and C29 ketone (99.8% and 92% decreases, respectively), both deriving from the C29 alkane (Fig. 3A). *CER1* inactivation also affected the C27 and C31 alkane amounts, while the other minor alkanes were almost not affected. Compared with alkanes and their derivatives, the other wax component contents were only very slightly affected (Table I; Supplemental Fig. S1). *CER1* overexpression in the *cer1-1* background rescued wax biosynthesis (91% of the waxes of wild-type plants; Fig. 3A). The *CER1ox1* and *CER1ox2* lines showed an increase of the wax load (24% and 32% increases, respectively), largely manifested as an increase in the total alkane amount (87% and 101% increases, respectively), which was largely due to the increase in the C29 alkane amount (97% and 111% increases, respec-

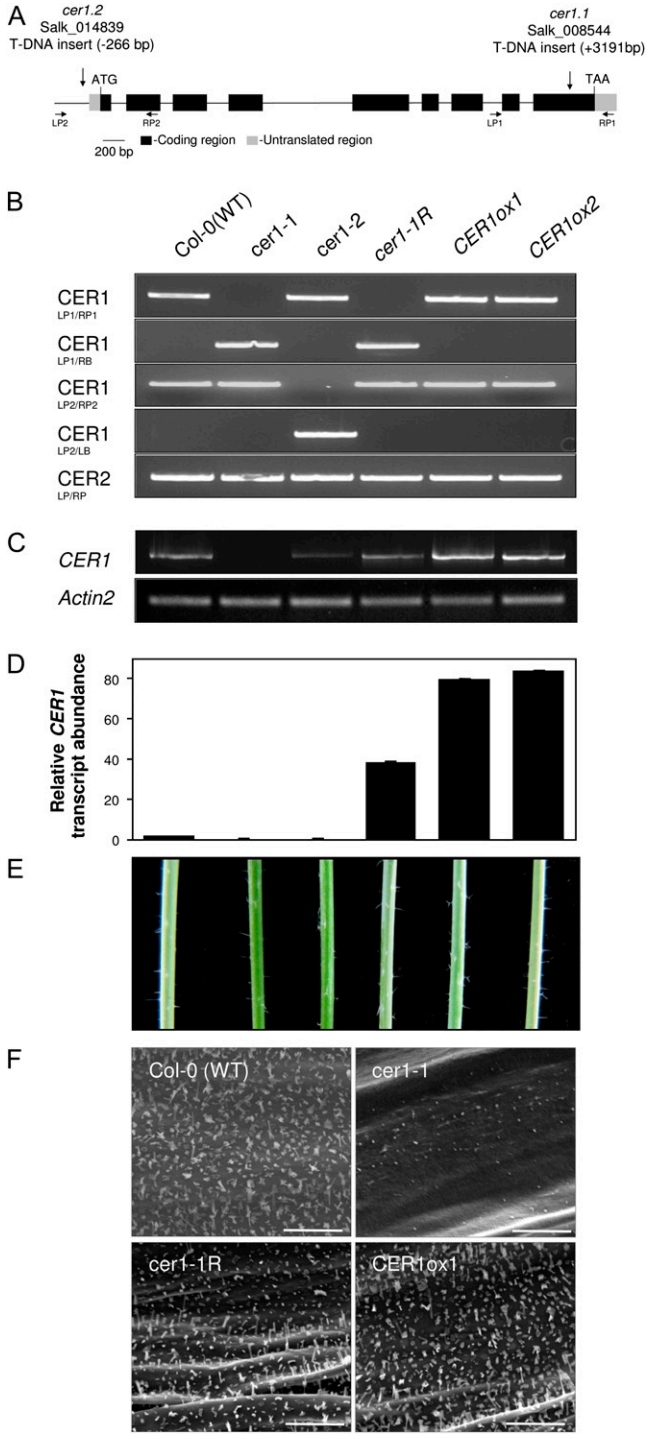


Figure 2. Molecular and phenotypic characterization of *cer1* mutants and *CER1*-overexpressing lines. A, Schematic of *CER1* gene structure indicating the positions of the T-DNA inserts in *cer1* mutant alleles. Dark boxes indicate exons, black lines indicate introns, and gray boxes indicate 5′ and 3′ untranslated regions. The arrows underneath the gene structure are the positions of convergent primers used for PCR on genomic DNA. B, PCR on genomic DNA of wild-type Col-0 (WT) plants, *cer1-1* and *cer1-2* mutants, the *cer1-1R* rescued line, and *CER1ox1* and *CER1ox2* overexpressing lines. Amplification of the *CER2* gene was used as a positive control. C, Semiquantitative RT-PCR analysis of steady-state *CER1* transcripts in 4-week-old plants of the different lines compared with the wild-type plants as indicated above. The *Actin2* gene was used as a constitutively expressed control. D, Real-time RT-PCR analysis of *CER1* gene expression in 4-week-old plants of the different lines compared with wild-type plants as indicated above. Results are presented as relative transcript abundance. The data represent means ± SD of three replicates. E, Stems from 6-week-old *cer1-1* and *cer1-2* mutants showing glossy phenotypes compared with wild-type plants, the *cer1-1R* rescued line, and *CER1ox1* and *CER1ox2* overexpressing lines. F, Epicuticular wax crystal formation on Arabidopsis wild-type (Col-0), *cer1-1*, *cer1-1R*, and *CER1ox1* stem surfaces detected by scanning electron microscopy at 5,000× magnification. Bars = 10 μm.

tively; Fig. 3A). *CER1* overexpression strongly affected the odd-carbon-numbered alkanes and mainly the C27, C29, and C31 alkanes; the even-carbon-numbered alkanes were almost not modified. Despite the strong increase in alkane amounts, the secondary alcohol and ketone levels slightly decreased as compared with the wild-type plants (around 10% and 40% decreases, respectively), suggesting that the alkane hydroxylase activity could be limiting. Interestingly, the aldehyde amount was increased in the three overexpressing lines compared with wild-type plants (67%, 98%, and 100% increases, respectively), which was mainly due to the increase in C28 and C30 aldehydes (Table I; Supplemental Fig. S1). In contrast, fatty acid, primary alcohol, isoalcohol, and ester amounts were only slightly modified in the different overexpressing lines compared with wild-type plants (Table I).

In leaves, the wax load per unit of leaf area of the *cer1-1* and *cer1-2* alleles was significantly reduced compared with wild-type plants (56% and 44% decreases, respectively), the *cer1-1* allele being again more affected than the *cer1-2* allele (Fig. 3B; Table II). This was largely due to a decrease of the alkane amount, which accounts for 60% of the total leaf wax load in wild-type plants. This modification was largely due to a decrease of the odd-carbon-numbered alkane amount (79% and 73% decreases, respectively) and, more precisely, the C29, C31, and C33 alkane contents (around 90% decrease). The other alkanes and other wax components were only weakly affected. *CER1* overexpression in the *cer1-1* background rescued the biosynthesis of waxes and led to a strong increase of the wax load (208% increase) in a similar way to what is found in *CER1ox1* and *CER1ox2* lines (307% and 312% increases, respectively; Fig. 3B). This was largely manifested as increases in the odd-carbon-numbered alkane amounts (340%, 481%, and 483% increases in *cer1-1R*, *CER1ox1*, and *CER1ox2*, respectively), mainly the C27, C29, C31, and C33 alkane contents. Interestingly, there was also a large increase of the isoalkane (2-methyl alkane) amounts in these lines (989%, 1,339%, and 1,495% increases, respectively), manifested as increases in the C29 and C31 isoalkane amounts. In contrast, other component amounts were poorly affected in the different overexpressing lines

Table I. *Cuticular wax composition of inflorescence stems of Arabidopsis Col-0, cer1-1, cer1-2, cer1-1R, CER1ox1, and CER1ox2 lines*

Mean values (μg dm^{-2}) of total wax loads and coverage of individual compound classes are given with SD (n = 4). The sums include shorter chain length constituents not presented in Figure 3.

Plant	Cuticular Wax Composition of Inflorescence Stems								
	Total Load	*n*-Alkanes	2-Alcohols	Ketones	1-Alcohols	Isoalcohols	Aldehydes	Fatty Acids	Esters
Col-0	1,305.6 ± 79.3	527.1 ± 34.6	133.2 ± 10.7	322.9 ± 28.2	162.7 ± 10.8	9.0 ± 2.2	69.9 ± 16.1	9.8 ± 3.0	71.0 ± 7.6
cer1-1	176.4 ± 17.2	48.7 ± 4.4	3.2 ± 1.0	1.1 ± 0.6	42.3 ± 4.4	5.5 ± 1.9	32.0 ± 4.2	2.8 ± 0.6	40.4 ± 3.9
cer1-2	325.4 ± 31.6	67.1 ± 6.5	7.8 ± 3.5	24.3 ± 10.3	92.0 ± 10.1	7.5 ± 1.2	46.6 ± 6.5	3.4 ± 0.5	76.8 ± 4.8
cer1-1R	1,193.4 ± 49.6	525.9 ± 30.0	93.5 ± 6.6	252.5 ± 6.3	101.2 ± 11.2	8.5 ± 1.3	117.0 ± 17.7	13.0 ± 2.7	82.0 ± 4.1
CER1ox1	1,615.0 ± 77.6	986.4 ± 50.7	116.2 ± 21.6	186.2 ± 26.0	108.9 ± 7.3	10.2 ± 2.6	139.7 ± 13.3	7.2 ± 1.1	60.7 ± 4.5
CER1ox2	1,720.6 ± 96.2	1,057.5 ± 95.4	124.9 ± 14.5	197.4 ± 18.0	116.8 ± 8.2	8.6 ± 2.4	138.4 ± 18.2	8.4 ± 1.8	68.6 ± 4.4

compared with wild-type plants (Table II; Supplemental Fig. S2).

Because wax components are issued from acyl-CoAs, the acyl-CoA pool was extracted from young stems and leaves of the wild-type, *cer1-1*, and *CER1ox1* lines and analyzed. We did not observe any significant modification of the acyl-CoA profile including VLC acyl-CoAs (Supplemental Fig. S3), suggesting that *CER1* ectopic expression did not affect the VLCFA elongation process.

Waxes are part of the cuticle and derived, as cutin monomers, from fatty acid precursors; thus, the cutin polyester of stems and leaves from the different lines was extracted and the cutin composition was analyzed in detail. Interestingly, stem and leaf cutin composition was quite similar between the different lines, demonstrating that ectopic *CER1* expression did not result in cutin biosynthesis perturbation (Supplemental Fig. S4).

Furthermore, we checked if the alkane production modifications could affect the cellular fatty acyl chain content. For that purpose, cuticular waxes of wild-type, *cer1-1*, and *CER1ox1* stems and leaves were first removed and then the total fatty acyl chain content was analyzed. Whatever the analyzed line, no modification of the cellular fatty acyl chain profile was observed (Supplemental Fig. S5). It should be pointed out that neither alkanes nor potential alkane precursors were detected in the *CER1*-overexpressing line extracts, suggesting that alkanes, despite their overproduction in this line, were correctly exported to the epidermis surface.

CER1 Deregulation Affects Plant Growth and Development

To assay the potential effects of the alkane production modifications on plant development, the growth of the different *CER1* lines was monitored. The *cer1-1* mutants were similar in all aspects to wild-type plants (Fig. 4A; Table III), except that the mutant stems were glossy due to the lack of wax (Fig. 2E). Moreover, as in the case of reported *cer1* mutants (Aarts et al., 1995), the *cer1-1* mutant exhibited a severe conditional male sterility in a low-humidity environment, which was linked to reduced pollen viability (Preuss et al., 1993). Fertility could be rescued in a high-humidity environment (Fig. 4B). Interestingly, *cer1-2* was fertile in an atmosphere of low humidity, whereas stems were glossy, suggesting that the residual *CER1* transcription in the *cer1-2* mutant is sufficient for normal fertility but not for normal stem wax biosynthesis. Organ fusions that were described in the *cer3* mutant (Chen et al., 2003; Kurata et al., 2003) or several cutin-deficient mutants (Wellesen et al., 2001; Kurdyukov et al., 2006a, 2006b) were never observed in *cer1-1* and *cer1-2* mutants. In contrast, *cer1-1R* and mainly *CER1ox1* and *CER1ox2* lines showed leaf growth retardation compared with wild-type plants (Fig. 4A; Table III). To define the characteristics of the different lines, wild-type, *cer1-1*, and *CER1ox1* plants were cultivated in the automated phenotyping platform PHENOPSIS, which was designed for the strict control of environmental conditions (Granier et al., 2006). The analysis of the three lines was performed by measuring several mor-

Table II. *Cuticular wax composition of rosette leaves of Arabidopsis Col-0, cer1-1, cer1-2, cer1-1R, CER1ox1, and CER1ox2 lines*

Mean values (μg dm^{-2}) of total wax loads and coverage of individual compound classes are given with SD (n = 4). The sums include shorter chain length constituents not presented in Figure 3.

Plant	Cuticular Wax Composition of Rosette Leaves							
	Total Load	*n*-Alkanes	Isoalkanes	1-Alcohols	Isoalcohols	Aldehydes	Fatty Acids	Esters
Col-0	74.9 ± 5.1	45.2 ± 2.4	1.4 ± 0.4	7.6 ± 1.3	5.5 ± 0.9	10.7 ± 1.2	3.5 ± 0.8	1.1 ± 0.2
cer1-1	32.4 ± 1.9	9.5 ± 0.7	1.5 ± 0.3	8.2 ± 0.7	4.2 ± 0.5	5.9 ± 0.4	2.5 ± 0.7	0.6 ± 0.1
cer1-2	40.8 ± 2.2	12.0 ± 1.0	1.4 ± 0.3	6.2 ± 0.8	7.4 ± 1.0	9.3 ± 0.9	3.5 ± 0.8	0.9 ± 0.1
cer1-1R	230.9 ± 12.6	198.6 ± 8.3	15.4 ± 1.2	6.0 ± 0.8	3.8 ± 0.5	4.5 ± 0.5	2.0 ± 0.2	0.7 ± 0.2
CER1ox1	304.8 ± 11.6	262.3 ± 9.7	20.4 ± 2.7	6.5 ± 0.5	3.5 ± 0.4	7.5 ± 0.7	2.7 ± 0.9	0.8 ± 0.1
CER1ox2	309.0 ± 19.8	263.2 ± 7.9	22.6 ± 1.8	7.2 ± 0.5	3.8 ± 0.6	9.1 ± 0.8	3.0 ± 0.3	1.2 ± 0.3

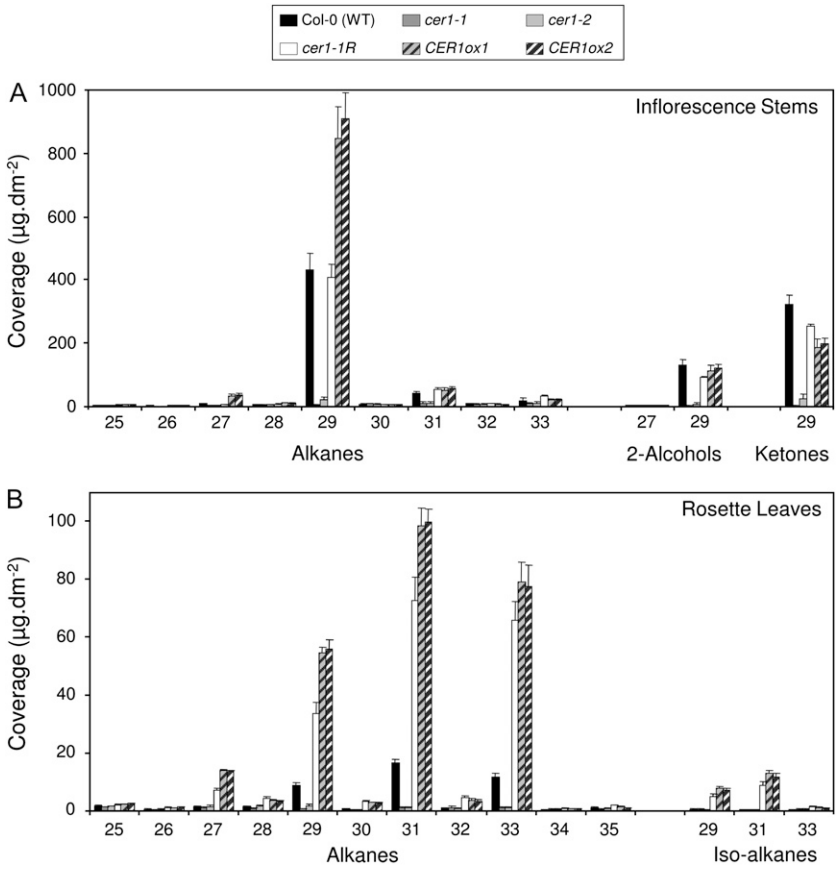


Figure 3. Cuticular wax composition of *cer1* mutants and *CER1*-overexpressing lines. A, Cuticular wax composition of inflorescence stems of wild-type Col-0 (WT), *cer1-1*, *cer1-2*, *cer1-1R*, *CER1ox1*, and *CER1ox2* lines. B, Cuticular wax composition of rosette leaves of Col-0, *cer1-1*, *cer1-2*, *cer1-1R*, *CER1ox1*, and *CER1ox2* lines. Amounts of major components are expressed as μg dm^{-2} stem or leaf surface area. Each wax constituent is designated by carbon chain length and is labeled by chemical class along the *x* axis. The data represent means ± SD of four replicates.

phological and anatomical traits in optimal plant growth conditions (well watered; Tables III and IV). When compared with the wild-type plants, the *cer1-1* mutant did not show significantly different leaf growth variables. On the contrary, the *CER1ox1* line analysis showed that these plants tended to flower earlier than wild-type plants (32.3 d versus 35.5 d). However, the morphology of buds and flowers was not affected in the *CER1ox1* line. Furthermore, the rosette leaf number, the rosette leaf area, and the leaf 6 area and thickness were lower at flowering in *CER1ox1* plants as compared with wild-type plants. Moreover, fresh and dry weights of *CER1ox1* plants at bolting were significantly lower than those of wild-type plants; however, the ratio between fresh and dry weights was the same. Interestingly, the *CER1ox1* leaf 5 foliar index tended to be lower as compared with the wild-type index, indicating a modification of the general leaf shape in these growth conditions. A detailed analysis of leaf 6 adaxial side cells was performed, showing that the stomatal index was not modified in the different lines (Table IV). Nevertheless, the epidermal cell analysis showed that the *CER1ox1* line had smaller cells compared with wild-type plants. The epidermal cell density was slightly increased in the *CER1ox1* line but did not compensate for the decrease in size, resulting in smaller leaves. These results suggested that leaf epidermal cell division and expansion were impaired in the *CER1*-overexpressing line.

CER1 Expression Is Modulated at the Transcriptional Level under Abiotic Stress Conditions

Wax production and export in aerial parts of the plants are known to be modulated by different environmental factors such as light, freezing temperatures, or water deficiency (Shepherd and Wynne Griffiths, 2006; Panikashvili et al., 2007; Joubès et al., 2008; Kosma et al., 2009). To assay the potential environmental regulation of *CER1* expression, we quantified *CER1* transcripts in 15-d-old seedlings exposed to different stress conditions (Table V) in comparison with *RD29A* transcripts used as a control for treatment efficiency. Dark and cold treatments resulted in a decreased expression of the *CER1* gene, whereas when plants were placed in the light for 8 h after 24 h of dark treatment or at 22°C for 24 h after 24 h of cold treatment, *CER1* transcripts were significantly increased, indicating that *CER1* transcription is negatively regulated by cold and dark stress. Treatment of the plants with different concentrations of NaCl or mannitol for 24 h resulted in an increase of *CER1* transcript levels as compared with the untreated plants. We also analyzed the modulation of *CER1* expression when plants were exposed to low-humidity conditions for 24 h (Fig. 5A). Dehydration led to an increase of the relative abundance of *CER1* transcripts by 40-fold for up to 6 h before decreasing. After 24 h of exposure to low-humidity conditions, *CER1* transcript level was still 20 times

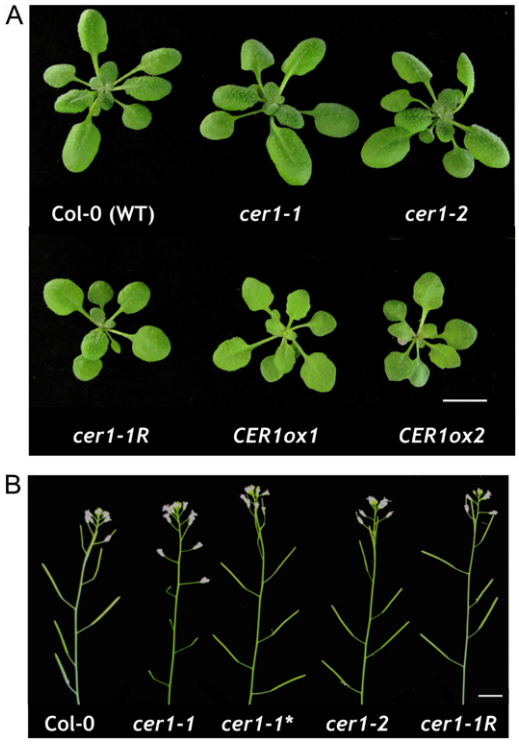


Figure 4. Phenotypes of *cer1* mutants and *CER1*-overexpressing lines. A, Phenotypes of 4-week-old rosettes of wild-type Col-0 (WT), *cer1-1*, *cer1-2*, *cer1-1R*, *CER1ox1*, and *CER1ox2* lines. B, The *cer1-2* mutant is fertile in normal conditions, whereas the *cer1-1* mutant shows conditional male sterility that can be restored in high-humidity conditions (*cer1-1**) or by functional complementation (*cer1-1R*). Bars = 1 cm.

higher than in the control. From these observations, we conclude that transcriptional control plays a major role in the regulation of CER1 during water stress.

Because *CER1* gene expression was found to be regulated by osmotic stresses, we examined whether abscisic acid (ABA) could have an effect on *CER1* transcript abundance. The ABA treatments resulted in a large increase of *CER1* transcript level, which was proportional to the ABA concentration and higher than the increase of *RD29A* transcript level (Fig. 5B). Treatment with 100 μM ABA led to a 350- fold increase of *CER1* transcript abundance compared with the mock-treated plants. We also analyzed *CER1* gene expression in time-course studies when plants were submitted to 10 μM ABA treatment for 24 h. ABA treatment led to a modification of the relative abundance of *CER1* transcripts, with an increase by a factor of 270 for up to 4 h (Fig. 5C). To confirm the transcriptional induction of the *CER1* gene in response to ABA, seeds of plants containing the *ProCER1*:*GUS* construct were germinated on control medium. After 2 weeks, 10 or 100 μM ABA was added to the medium for 24 h and plants were assayed for GUS activity, which was clearly induced by the ABA treatment (Fig. 5D). To investigate whether this effect could be specific, 15-d-old plants were treated with different hormones such as ABA, GA_3, methyl jasmonate (MeJa), salicylic acid (SA), cytokinin (BAP), and auxin (picloram) for 4 and 24 h (Table V). Only ABA had a significant impact on *CER1* expression, demonstrating that the phytohormone played an important role in the transcriptional control of *CER1* activation.

CER1 Deregulation Affects Cuticle Properties and Response to Soil Water Deficit

Because cuticle properties are crucial for the control of water movement between the epidermis cell and the atmosphere, we assessed the impact of VLC alkane biosynthesis modifications on leaf cuticle properties by measuring chlorophyll-leaching and water-loss rates on wild-type, *cer1-1*, and *CER1ox1* lines grown in control conditions (Fig. 6, A and B). The *cer1-1* mutant showed a higher rate of both leaf water loss and chlorophyll leaching than wild-type plants, whereas *CER1ox1* plants showed a lower rate of both water loss and chlorophyll leaching than wild-type plants. From these analyses, we concluded that the *cer1-1* mutant showed increased cuticle permeability, whereas the VLC alkane-overproducing *CER1ox1* line clearly showed reduced cuticle permeability.

To determine to what extent the modification of cuticle properties affects the plant response to soil water deficit, the morphological and anatomical traits of wild-type, *cer1-1*, and *CER1ox1* lines were measured in controlled moderate, continuous soil water deficit conditions (water deprivation; Table III) and compared with traits measured in optimal plant growth conditions (well watered; Table III). Soil water deficit led to a significant decrease of all growth parameters: plants were smaller with fewer leaves, and leaves were smaller and thinner. Fresh and dry weights were highly reduced. However, while wild-type plants and *cer1-1* mutants showed the same modifications of growth and morphological traits, *CER1ox1* whole plant and leaf traits were less modified in response to water deficit compared with wild-type plants. For instance, biomass was reduced by around 75% in wild-type plants but only by 24% in *CER1ox1* plants. These results suggested that the *CER1ox1* line was better able to sustain growth under soil water deficit conditions than wild-type plants and *cer1-1* mutants. The different lines were then tested for their susceptibility to severe soil water deficit conditions (Fig. 6C). Wild-type, *cer1-1*, and *CER1ox1* lines were grown under optimal conditions for 3 weeks, then plants were deprived of water until wild-type plants wilted and showed a relative water content (RWC) of 48% compared with well-watered plants, which maintained a RWC of 90% (Fig. 6D). After this 20-d treatment, *cer1-1* plants wilted and reached a RWC of 23%. In contrast, *CER1ox1* plants showed a less sensitive phenotype compared with wild-type and *cer1-1* lines. Indeed, after the stress period, *CER1ox1* plants stayed turgid and maintained a higher RWC of 77% compared with wild-type and *cer1-1* plants. These data suggested that

Table III. *Growth and morphological traits of Arabidopsis Col-0, cer1-1, and CER1ox1 lines*

The plants were in well-watered (WW; 0.35 g water g^{-1} dry soil) and water-deprived (WD; 0.20 g water g^{-1} dry soil) conditions. The data represent means ± SD (n = 4–12) for each trait. Different letters indicate significant differences among means using the nonparametric test of Kruskal-Wallis for multiple comparisons ($P < 0.05$).

Genotype	Treatment	Growth and Morphological Traits							
		Days to Flowering	Rosette Leaf No.	Rosette Leaf Area	Leaf 6 Area	Leaf 6 Thickness	Leaf 5 Foliar Index	Fresh Weight at Bolting	Dry Weight at Bolting
				cm^2		μm		mg	
Col-0	WW	35.5 ± 2.4[a]	19.0 ± 2.0[a]	41.7 ± 8.5[a]	1.15 ± 0.30[a]	201.9 ± 9.3[a]	1.361 ± 0.056[a,b]	622.3 ± 221.5[a]	59.18 ± 21.78[a]
	WD	36.3 ± 1.0[a]	13.5 ± 0.6[b]	12.0 ± 2.7[b]	0.78 ± 0.27[b]	158.1 ± 12.7[c,d]	1.344 ± 0.070[a,b]	150.9 ± 45.5[b]	20.53 ± 8.50[b]
cer1-1	WW	35.8 ± 1.0[a,b]	19.8 ± 1.3[a]	43.0 ± 1.1[a]	1.21 ± 0.13[a]	203.0 ± 22.8[a]	1.431 ± 0.070[a]	730.5 ± 290.1[a]	70.13 ± 27.09[a]
	WD	35.0 ± 2.8[a,b]	13.5 ± 1.3[b]	10.6 ± 2.0[b]	0.69 ± 0.06[b]	169.7 ± 7.7[b,c]	1.290 ± 0.178[a,b]	186.3 ± 13.6[b]	23.75 ± 2.03[b]
CER1ox1	WW	32.3 ± 2.5[b]	11.8 ± 1.5[c]	10.9 ± 2.6[b]	0.62 ± 0.12[b]	175.7 ± 13.9[b]	1.268 ± 0.137[b]	78.3 ± 11.6[c]	7.25 ± 1.78[c]
	WD	32.8 ± 2.9[a,b]	10.0 ± 0.8[a]	3.8 ± 1.3[c]	0.35 ± 0.06[c]	156.6 ± 12.3[d]	1.296 ± 0.089[a,b]	59.7 ± 18.9[c]	8.38 ± 3.60[c]

cuticle modifications induced by *CER1* overexpression resulted in a significantly reduced susceptibility to soil water deficit.

CER1 Deregulation Influences Plant Pathogen Susceptibility

Because recent findings indicate that the cuticle plays an important role in the plant response to pathogens, the phenotypes of the *cer1-1* mutant and *CER1*-overexpressing lines were assessed and compared with wild-type plants in response to two types of pathogens: *Pseudomonas syringae* pv *tomato* (*Pst*), a hemibiotrophic bacterial pathogen, and *Sclerotinia sclerotiorum*, a necrotrophic fungal pathogen.

In response to the *Pst DC3000* virulent strain, spreading chlorosis was observed 3 d after inoculation in *CER1ox1* and *CER1ox2* leaves, while very few lesions were observed in wild-type or *cer1-1* leaves (Fig. 7A). During an incompatible-type interaction with *Pst DC3000/avrRpt2*, *CER1ox1* and *CER1ox2* lines showed a delay in the onset of the hypersensitive response, as compared with wild-type and *cer1-1* leaves, 2 d after inoculation (Fig. 7B). These observations suggest that *CER1* overexpression causes increased susceptibility and loss of resistance in response to *Pst* virulent and avirulent strains, respectively. Evaluation of in planta bacterial growth in these lines confirmed the increased susceptibility and reduced resistance of both *CER1ox* lines to *Pst* virulent and avirulent strains as compared with wild-type and *cer1-1* plants (Fig. 7, A and B). No significant quantitative difference was detected in the *cer1-1* mutant as compared with wild-type plants in response to *Pst*.

Several studies have underlined the role of the cuticle in response to necrotrophic fungi, so we tested the response of *cer1-1* and *CER1ox* lines to *Sclerotinia* (Fig. 7C). Plant leaves were inoculated with a paper disc covered with the mycelium (Perchepied et al., 2010) and placed at high humidity for 24 h for optimal development of the fungus. The resistance test was based on a semiquantitative evaluation of the progression of the fungus according to a predetermined disease index and scored 7 d after inoculation (Perchepied et al., 2010). To evaluate the resistance of *cer1-1* and *CER1ox* lines, the susceptible ecotype Shahdara and the resistant ecotype Rubezhnoe-1 were used as controls. The results revealed that the *cer1-1* mutant was slightly more susceptible than wild-type plants and the resistant ecotype Rubezhnoe-1, whereas both *CER1ox1* and *CER1ox2* lines were significantly more susceptible than wild-type plants or the *cer1-1* mutant and intermediate compared with the resistant (Rubezhnoe-1) and susceptible (Shahdara) ecotypes (Fig. 7C).

Table IV. *Anatomical traits of Arabidopsis Col-0, cer1-1, and CER1ox1 lines*

The plants were in well-watered (WW; 0.35 g water g^{-1} dry soil) and water-deprived (WD; 0.20 g water g^{-1} dry soil) conditions. The data represent means ± SD (n = 4–12) for each trait. Different letters indicate significant differences among means using the nonparametric test of Kruskal-Wallis for multiple comparisons ($P < 0.05$).

Genotype	Treatment	Anatomical Traits: Adaxial Epidermal Cells			Anatomical Traits: Adaxial Stomatal Cells		
		Cell Density	Estimated Cell Size	Estimated Cell No.	Stomatal Density	Stomatal Index	Estimated Stomata No.
		cells mm^{-2}	μm^2	*cells leaf* $^{-1}$	*stomata* mm^{-2}	*% stomata cell* $^{-1}$	*stomata leaf* $^{-1}$
Col-0	WW	238.4 ± 30.8[b]	4,531 ± 955[a,b]	25,722 ± 5,684[a]	95.2 ± 16.2[d]	18.10 ± 0.89[a]	9,565 ± 2,258[a,b]
	WD	308.2 ± 41.8[a]	3,345 ± 289[c]	22,971 ± 6,028[a,b]	121.7 ± 23.7[a,b]	17.99 ± 1.01[a]	10,054 ± 3,054[a,b]
cer1-1	WW	240.7 ± 39.5[b]	4,881 ± 791[a]	25,414 ± 5,427[a]	105.5 ± 17.1[c,d]	18.94 ± 1.16[a]	11,219 ± 1,150[a]
	WD	347.3 ± 52.1[a]	3,277 ± 311[c]	21,197 ± 240[a,b]	138.8 ± 26.6[a]	18.12 ± 1.14[a]	8,215 ± 1,308[b,c]
CER1ox1	WW	255.3 ± 30.1[b]	3,999 ± 239[a,b]	15,606 ± 3,612[b,c]	109.3 ± 15.1[b,c]	18.71 ± 0.95[a]	6,614 ± 2,106[c,d]
	WD	308.6 ± 41.6[a]	3,718 ± 489[c]	9,480 ± 550[c]	128.9 ± 19.8[a]	18.52 ± 0.69[a]	4,040 ± 277[d]

Table V. *Modulation of CER1 expression in 15-d-old Arabidopsis seedlings subjected to different stress conditions*

The gene expression level was determined by real-time RT-PCR analysis. Results are presented as relative transcript abundance, and the relative transcript abundance of the gene of interest in the control sample was arbitrarily defined as 1. The abiotic stress-inducible *RD29A* gene was used as a control for treatment efficiency. The data represent means ± SD of three replicates.

Treatment		Relative Transcript Abundance		Treatment	Relative Transcript Abundance	
		CER1	*RD29A*		*CER1*	*RD29A*
Dark	Control	1.00 ± 0.17	1.00 ± 0.12	Hormones		
	Dark, 24 h	0.02 ± 0.00	0.01 ± 0.00	Control	1.00 ± 0.40	1.00 ± 0.09
	Recovery, light, 8 h	1.32 ± 0.48	0.67 ± 0.18	MeJa, 4 h (100 μM)	0.60 ± 0.11	0.70 ± 0.08
	Dark, 48 h	0.02 ± 0.00	0.01 ± 0.00	MeJa, 24 h	7.81 ± 0.21	2.51 ± 0.81
Cold	Control	1.00 ± 0.17	1.00 ± 0.12	SA, 4 h (1 mM)	1.12 ± 0.22	0.14 ± 0.04
	4°C, 24 h	0.08 ± 0.02	5.96 ± 1.14	SA, 24 h	1.62 ± 0.39	1.75 ± 0.40
	Recovery, 22°C, 24 h	0.64 ± 0.05	0.26 ± 0.01	Picloram, 4 h (10 μM)	0.75 ± 0.14	0.26 ± 0.08
	4°C, 48 h	0.16 ± 0.05	0.91 ± 0.12	Picloram, 24 h	29.14 ± 4.38	4.10 ± 1.08
NaCl	Control	1.00 ± 0.08	1.00 ± 0.03	GA_3, 4 h (50 μM)	1.52 ± 0.32	0.25 ± 0.05
	50 mM, 24 h	2.31 ± 0.11	7.46 ± 0.35	GA_3, 24 h	5.98 ± 1.10	0.86 ± 0.12
	100 mM, 24 h	3.71 ± 0.29	45.89 ± 3.22	BAP, 4 h (50 μM)	1.53 ± 0.69	0.34 ± 0.07
	150 mM, 24 h	6.77 ± 0.14	79.89 ± 2.88	BAP, 24 h	10.93 ± 3.75	0.72 ± 0.11
Mannitol	Control	1.00 ± 0.10	1.00 ± 0.68	ABA, 4 h (10 μM)	47.84 ± 14.95	36.76 ± 2.31
	150 mM, 24 h	2.01 ± 0.49	6.11 ± 041	ABA, 24 h	171.85 ± 20.54	29.75 ± 6.48
	300 mM, 24 h	2.99 ± 0.10	23.67 ± 3.96			

DISCUSSION

CER1 Is Strongly Associated with Wax VLC Alkane Biosynthesis

We showed that *CER1* belongs to a family of four genes but is the only one that is significantly expressed in vegetative organs and coexpressed with both *CER3* and *MAH1* genes, in accordance with its putative role in the alkane-forming pathway (Chen et al., 2003; Kurata et al., 2003; Greer et al., 2007). Moreover, *CER1* expression is strongly confined to the epidermis cell layer, suggesting that its primary function is linked to cuticular wax production, as has been demonstrated for several genes involved in VLCFA biosynthesis (Kunst et al., 2000; Hooker et al., 2002; Efremova et al., 2004; Joubès et al., 2008), in wax production (Rowland et al., 2006; Greer et al., 2007; Li et al., 2008), or in transport (Pighin et al., 2004; Panikashvili et al., 2007; Debono et al., 2009). Our expression data also showed that both *CER1* and *CER1-like1* are expressed in reproductive organs participating in wax biosynthesis in flowers and fruits. However, the conditional male sterility of the *cer1-1* null allele suggests that the function of both proteins is not redundant. Indeed, the tryphine that coats the pollen grain surface contains significant quantities of VLC alkanes and their derivatives, which are crucial for pollen viability (Preuss et al., 1993; Aarts et al., 1995; Mayfield and Preuss, 2000). Waxes are also involved in pollen-stigma recognition, imbibition of the pollen grain on the stigmatic papillae, or the dehiscence processes (Aarts et al., 1995; Hülskamp et al., 1995; Hooker et al., 2002; Joubès et al., 2008). Moreover, expression of *CER1* in petals could suggest a role of VLC alkanes in their hydrophobic properties called the "petal effect" (Feng et al., 2008). The fact that *CER1*, *CER3*, and *MAH1* are highly expressed in reproductive organs suggests an important role for the alkane-forming pathway components in the reproduction processes.

Analysis of *CER1* transgenic plants showed a strict correlation between *CER1* ectopic expression and wax VLC alkane production without other metabolic defects in cutin, acyl-CoA, and intracellular fatty acyl chain profiles. We demonstrated that *CER1* overexpression increased specifically the odd-carbon-numbered alkanes, mainly C27, C29, C31, and C33 alkanes, with only minor modifications of other wax components. Surprisingly, *CER1ox* lines showed a substantial accumulation of iso-branched alkanes in leaves, where they are normally only found in trace amounts, suggesting that CER1 in the context of the *CER1ox* lines is probably able to produce methyl alkanes from methyl VLCFAs. From these analyses, we conclude that CER1 is the enzyme controlling alkane biosynthesis with a high substrate specificity, leading exclusively to alkane and isoalkane formation and a high chain length specificity manifested as the increase of specific odd-carbon-numbered VLC alkanes. Although a lot of biochemical studies that addressed wax biosynthesis have tried to describe the alkane-forming pathway (Samuels et al., 2008), the biochemical details of plant VLC alkane biosynthesis have not been so far elucidated. The main hypothesis that has been proposed to explain the reaction leading from VLCFA precursors to VLC alkanes suggests that VLCFAs are reduced to intermediate VLC aldehydes, which are then converted to VLC alkanes by decarbonylation. This hypothesis is supported by numerous analyses that have been carried out with the goal of characterizing CER1 activity (Cheesbrough and Kolattukudy, 1984; Dennis and Kolattukudy, 1992; Schneider-Belhaddad and Kolattukudy, 2000); nevertheless, the final biochemical proof for decarbonylation

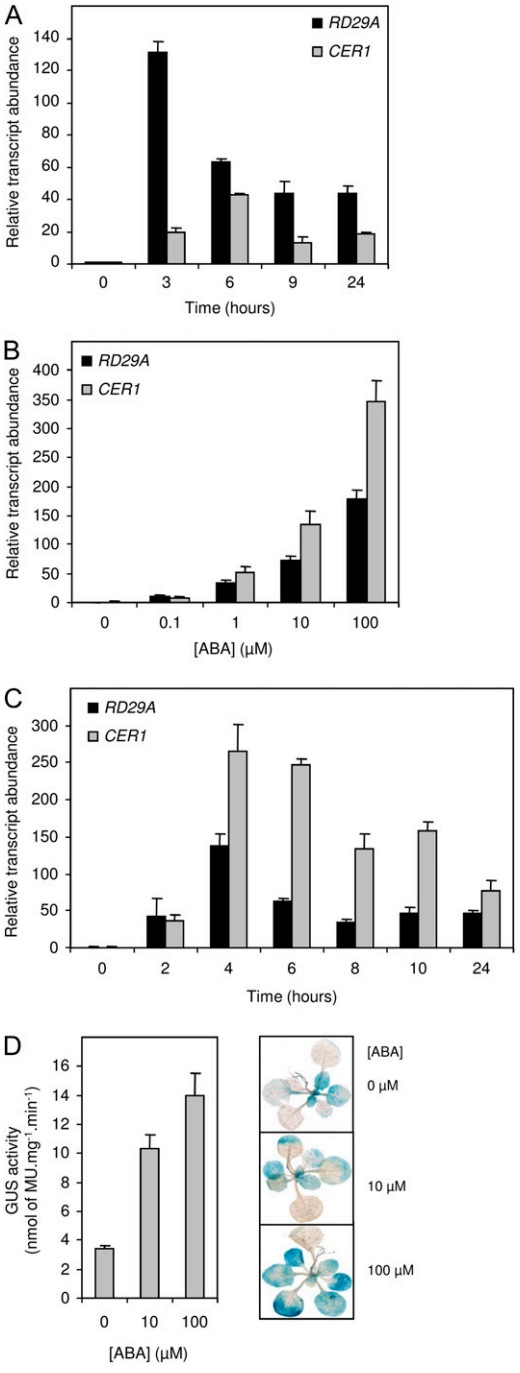


Figure 5. Modulation of *CER1* expression in Arabidopsis seedlings subjected to stress conditions. A, Modulation of *CER1* expression in plants exposed to low-humidity conditions for 24 h. B, Modulation of *CER1* expression in plants exposed to different ABA concentrations for 24 h. C, Time-course analysis of *CER1* expression in plants exposed to 10 μM ABA for 24 h. *RD29A* gene expression was used as a control for treatment efficiency. The gene expression level was determined by real-time RT-PCR analysis. Results are presented as relative transcript abundance. The data represent means ± SD of three replicates. D, Quantitative assay and histochemical staining revealed induction of the GUS reporter activity in a 2-week-old *ProCER1:GUS* transgenic line exposed to different ABA concentrations for 24 h. The data represent means ± SD of four replicates. MU, Methylumbelliferone.

is currently missing. To characterize the CER1 activity, we and other groups performed analyses using yeast as a heterologous system. This system was shown to be very useful to analyze the catalytic activity of wax-related enzymes such as VLCFA-producing KCSs (Joubès et al., 2008), the wax synthase WSD1 (Li et al., 2008), or, more recently in our hands, the alcohol-forming FARs (Domergue et al., 2010). Expressing CER1 alone or with other proteins involved in VLCFA and wax biosynthesis never led to alkane or aldehyde production (data not shown). Using chemically synthesized C30 aldehydes and other potential CER1 VLC substrates, we also tried yeast-feeding experiments as well as in vitro assays to improve the solubility and availability of these molecules, but none of these strategies resulted in any conclusive results. Since CER1 chain length specificity results in the production of alkanes longer than C27 and as yeast does not produce VLCFAs longer than C26, we then expressed CER1 in the yeast strain engineered by Denic and Weissman (2007) to produce up to C30 VLCFAs. Nevertheless, although C30 fatty acids could be detected, no other products that could result from CER1 activity could be identified, suggesting that yeast may not be a suitable model for characterizing CER1 enzymatic activity. Therefore, we are currently developing biochemical and analytical approaches with the VLC alkane-overproducing *CER1ox1* Arabidopsis line in order to solve CER1 biochemical activity and plant VLC alkane biosynthesis.

The Role of Wax VLC Alkanes in Abiotic Stress Response

Waxes are known to play important general functions in interactions of plants with their environment. One major cuticle function is to prevent unregulated water loss, which is especially important for plant survival in water-limited environments (Kerstiens, 1996; Kosma and Jenks, 2007). Indeed, Arabidopsis plants exposed to water deficit treatment exhibit a significant increase in the amount of total leaf wax, mainly due to a dramatic increase in VLC alkane amount, suggesting that alkane synthesis is a key to this stress response (Kosma et al., 2009). As has been also reported in rose (*Rosa* × *hybrida* 'Poulpollo'; Jenks et al., 2001) and tree tobacco (*Nicotiana glauca*; Cameron et al., 2006), Arabidopsis wax increases under water deficit conditions lead to a less-water-permeable cuticle, an adaptation that limits transpiration during prolonged climatic drought (Kosma et al., 2009). In this paper, we showed that leaf wax VLC alkane modification, without apparent major cutin perturbation, can be associated with disturbed cuticle properties. Indeed, cuticle permeability was increased in the *cer1-1* mutant whereas it was reduced in the VLC alkane-overproducing *CER1ox1* line, resulting in reduced susceptibility to soil water deficit. Modifications of cuticle properties are known to deeply perturb plant water management. For instance, disorganized cuticle in wax- or cutin-deficient mutants increases both cu-

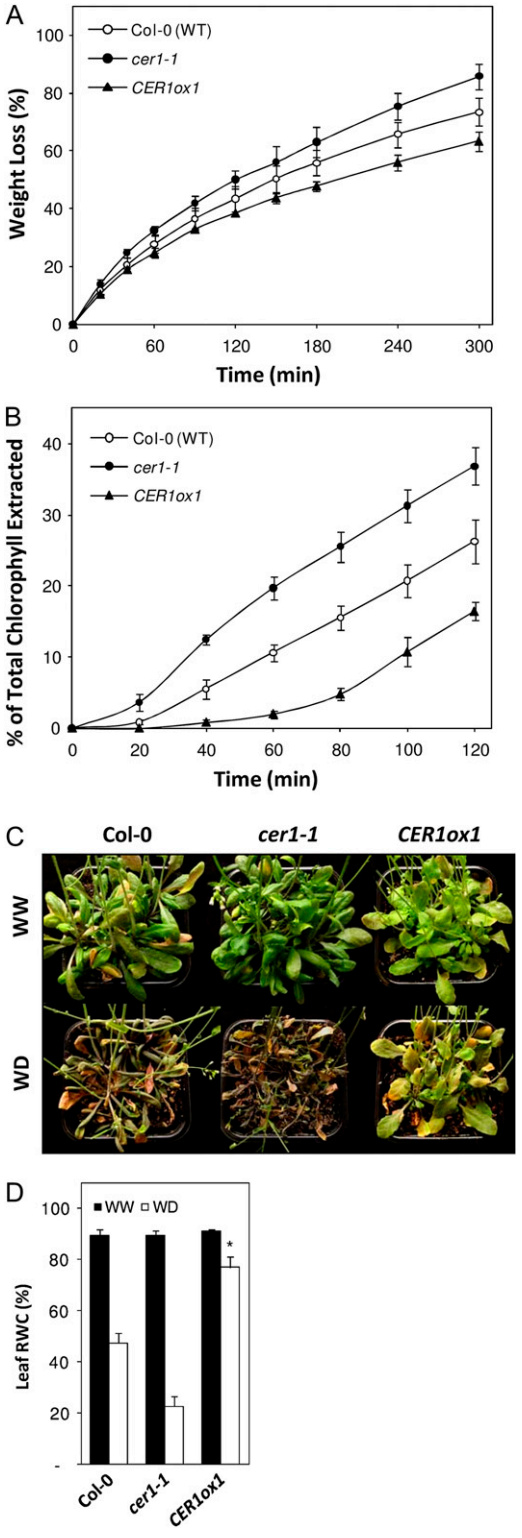


Figure 6. CER1 deregulation affects cuticle properties and response to soil water deficit. A, Water-loss rates (expressed as a percentage of initial water-saturated weight) of isolated rosettes from wild-type Col-0 (WT), *cer1-1*, and *CER1ox1* plants. Four-week-old plants were dark acclimated for 3 h, excised, and placed immediately in water in the dark for 1 h to equilibrate water contents. Rosette weights were determined gravimetrically using a microbalance. The data represent means ± SD of five replicates. B, Chlorophyll extraction rates (expressed as a percentage of total chlorophyll extracted after 24 h) of rosettes from Col-0, *cer1-1*, and *CER1ox1* plants. Four-week-old plants were dark acclimated for 3 h, and rosettes were immersed in 80% ethanol for 24 h. The data represent means ± SD of five replicates. C, Water soil deprivation experiment. Three-week-old plants were exposed to 20 d of water deprivation (WD) alongside well-watered plants (WW). D, Well-watered and water-deprived plants were used to determine leaf RWC. The data represent means ± SD of five replicates (the experiments were repeated once with similar results). Significance was assessed by Student's *t* test (* $P < 0.01$).

ticle permeability and transpiration, as in the *cer1-1* mutant (Chen et al., 2003; Schnurr et al., 2004; Li et al., 2007; Lü et al., 2009; Weng et al., 2010). In contrast, accumulation of leaf cuticular components through the overexpression of the SHINE- or LAS-type transcription factor in Arabidopsis or in alfalfa (*Medicago sativa*) led to a significant drought tolerance improvement (Aharoni et al., 2004; Zhang et al., 2005, 2007; Yang et al., 2011). Interestingly, these transgenic plants showed the same kind of developmental defects as the *CER1ox1* plants, which could suggest that the modifications of the leaf surface properties strongly perturbed the interactions of the epidermal cells with their environment, leading to leaf growth retardation. These findings support the notion that wax alkanes are important for plant water status control and water stress response.

At the transcriptional level, several genes encoding enzymes involved in wax biosynthesis are induced by osmotic stresses, *CER1* being the most induced gene (Hooker et al., 2002; Panikashvili et al., 2007; Joubès et al., 2008; Kosma et al., 2009). Furthermore, previous studies have demonstrated that several cuticle-associated genes are responsive to ABA, suggesting that this phytohormone is necessary to activate this set of genes in response to water deficit (Hooker et al., 2002; Duan and Schuler, 2005; Panikashvili et al., 2007; Kosma et al., 2009). We have also previously shown that ABA treatment induces wax production in leaves with a preferential increase in VLC alkanes (Kosma et al., 2009). In this paper, we clearly demonstrated that *CER1* expression is induced in response to osmotic and ABA stresses and that a rapid regulation of alkane biosynthesis may occur in these conditions, suggesting that wax production can be regulated daily or can change in a few hours. These data are in agreement with an atomic microscopic study using common snowdrop (*Galanthus nivalis*) that showed a regeneration of wax deposit at the leaf surface in less than 2 h (Koch et al., 2004). Collectively, our results demonstrate that *CER1* is an essential ABA-inducible cuticle-associated gene involved in VLC alkane production.

Role of Wax VLC Alkanes in Biotic Stress Response

Besides its role in abiotic stress tolerance, the cuticle is thought to play an important role in plant defense

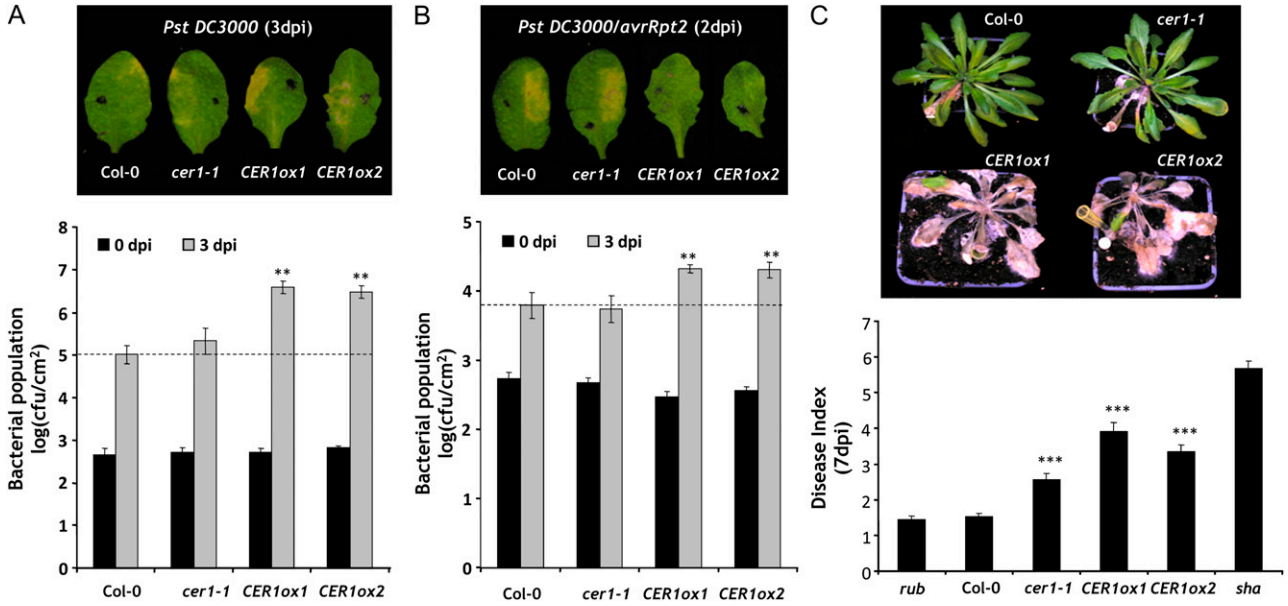


Figure 7. *CER1*-overexpressing lines show enhanced susceptibility to *Pst* and *Sclerotinia*. A, Phenotype of wild-type Col-0, *cer1-1*, *CER1ox1*, and *CER1ox2* lines 3 d post inoculation (dpi) with the *Pst DC3000* virulent strain at 5×10^5 colony-forming units (cfu) mL^{-1}. Growth of *Pst DC3000* in the different lines was measured at 0 d (black bars) and 3 d (gray bars) after inoculation performed with a bacterial suspension at 5×10^5 cfu mL^{-1}. B, Phenotypes of Col-0, *cer1-1*, *CER1ox1*, and *CER1ox2* lines 2 d after inoculation with the *Pst DC3000/avrRpt2* avirulent strain at 5×10^6 cfu mL^{-1}. Growth of *Pst DC3000/avrRpt2* in the different lines was measured at 0 d (black bars) and 3 d (gray bars) after inoculation performed with a bacterial suspension at 5×10^5 cfu mL^{-1}. C, Macroscopic observation of symptoms 7 d after inoculation with the *Sclerotinia* mycelium of Col-0, *cer1-1*, *CER1ox1*, and *CER1ox2* lines. Disease symptoms were scored 7 d after inoculation with the mycelium. The Arabidopsis ecotypes Shahdara (sha) and Rubezhnoe-1 (rub) were used as susceptible and resistant controls, respectively. The data represent average disease scores ± SD of three independent experiments. Significance was assessed by Student's *t* test (** $P < 0.05$, *** $P < 0.01$).

against pathogens. The cuticle is a physical barrier representing a constitutive defense against pathogens. Several recent studies suggest that the cuticle is also a dynamic structure including signaling circuits and effector molecules (Chassot et al., 2008; Reina-Pinto and Yephremov, 2009). Analysis of cuticle-defective mutants indicates that cuticle-derived signals act negatively on necrotrophic fungal infection and positively on biotrophic fungi and virulent bacterial pathogens (Xiao et al., 2004; Bessire et al., 2007; Tang et al., 2007; Raffaele et al., 2009). Our data indicate that the leaf VLC alkane depletion does not strongly interfere with the pathogen response, whereas *CER1* overexpression causes increased susceptibility to the hemibiotrophic bacterial pathogen *Pst* and the necrotrophic fungal pathogen *Sclerotinia*. Some information about the role of cuticle components in resistance to necrotrophic pathogens is now available. Increased resistance of Arabidopsis or tomato (*Solanum lycopersicum*) cutin-deficient mutants to *Botrytis cinerea* (Bessire et al., 2007; Chassot et al., 2007; Tang et al., 2007; Curvers et al., 2010) is thought to be due to a better perception of the fungal activity correlated to increased cuticle permeability. Indeed, cutin monomers released from the action of cutinase can act as elicitors that cross the cuticle barrier faster and trigger defense responses (Chassot et al., 2008). The *cer1-1* mutant does not exhibit any alteration of the cutin composition, which can explain that, despite the wax phenotype, *cer1-1* was not more resistant to *Sclerotinia* than wild-type plants. On the other hand, VLC alkane overproduction in *CER1ox* lines increases the susceptibility to *Sclerotinia*. The cuticle permeability modification in these transgenic plants could be responsible for a less efficient perception of the fungal elicitors, delaying the activation of the defense responses. Furthermore, it has been shown that leaf or fruit waxes could contain active components that induce germination and appressorium formation by fungal pathogens (Podila et al., 1993; Hegde and Kolattukudy, 1997; Reisige et al., 2006). Therefore, VLC alkanes accumulated on the *CER1ox* leaf surface could act as components activating the development of the fungus or could deeply perturb the hydrophobic properties of the leaf cuticle and allow better fungus propagation. On the contrary, the analysis of two cutin-deficient mutants, *att1* and *sma4/lacs2*, showed that cuticle-derived signals act positively on virulent bacterial pathogens, suggesting that normal cuticle is an effective barrier against these pathogens (Xiao et al., 2004; Tang et al., 2007). In this paper, we showed that wax VLC alkane accumulation on the *CER1ox* leaf surface enhances the plant susceptibility to *P. syringae*. We also previously showed that VLCFAs and VLCFA derivatives such as

sphingolipids are key molecules of the plant immune response to pathogen attacks by modulating the hypersensitive response (Raffaele et al., 2008). In contrast to the very low quantity of VLCFAs required for the sphingolipid biosynthesis in any plant cell (Markham and Jaworski, 2007), an important amount of VLCFAs is necessary for the synthesis of the cuticular waxes in epidermal cells. It is possible, therefore, that the high production of VLC alkanes in *CER1ox* line epidermis cells needs a sustained production of VLCFAs to feed the alkane-forming pathway, which might be sufficient to perturb the biosynthesis of specific sphingolipids involved in plant-pathogen interaction (Raffaele et al., 2009) and consequently the resistance response to pathogen attack.

In summary, our findings showed that modifications of *CER1* expression specifically affect VLC alkane content in a way that strongly supports the hypothesis that CER1 encodes the alkane-forming enzyme. Furthermore *CER1* expression is highly regulated by abiotic stresses and modifying *CER1* expression alters cuticle permeability, leading to differential responses to abiotic and biotic stresses. By controlling alkane formation, *CER1* appears as a key gene in cuticle metabolism.

MATERIALS AND METHODS

Plant Material and Growth Conditions

Arabidopsis (*Arabidopsis thaliana* Col-0) was used in all experiments. The following T-DNA insertion lines were obtained from the Arabidopsis Biological Resource Center (www.arabidopsis.org): SALK_008544 (*cer1-1*) and SALK_014839 (*cer1-2*). Arabidopsis plants were cultivated under optimal growth conditions as described previously (Joubès et al., 2008). The 15-d-old seedlings were exposed to different concentrations of ABA, mannitol, and NaCl for 24 h as described previously (Kosma et al., 2009). For kinetic analysis, 15-d-old seedlings were exposed to 10 μM ABA for 24 h and harvested at different time points. For hormone treatments, 15-d-old seedlings were exposed to 100 μM MeJa, 1 mM SA, 10 μM picloram, 50 μM GA_3, 50 μM BAP, and 10 μM ABA for 4 and 24 h. The seedlings grown on Murashige and Skoog medium were exposed to low temperature (4°C), darkness, and drought for 24 and 48 h. After 24 h of treatment, plants were used for RNA extraction.

Measurements of leaf growth variables in control and soil water deficit conditions were performed with the PHENOPSIS automated platform (Granier et al., 2006; Tisné et al., 2010). Two soil water contents were imposed (0.35 and 0.2 g water g^{-1} dry soil), corresponding to optimal plant growth and continuous, moderate water deficit conditions, respectively (Aguirrezabal et al., 2006). Plants were sown and grown under controlled conditions as described (Massonnet et al., 2010) at 21°C, 12-h-light/12-h-dark photoperiod, and 230 μmol m^{-2} s^{-1} photosynthetically active radiation. Four plants per genotype and treatment were harvested at flowering, and whole-plant and leaf traits were determined. Immediately after harvest, total leaf number and individual leaf areas were determined. The total rosette area was calculated as the sum of the individual leaf areas. Foliar index of leaf 5 was determined as leaf length-to-width ratio. Thickness of leaf 6 was measured with a linear variable displacement transducer at four to 10 points per leaf blade on each side of the central vein. Transparent replication films of the adaxial epidermis of leaf 6 were obtained after evaporation of a varnish spread on the leaf. The density of epidermal cells and stomatal cells was then determined by microscopy in three zones at the base, middle, and top of the leaf using image-analysis software (Optimas-Bioscan 6.1). Stomatal index was calculated as stomatal cells/(stomatal cells + 2× stomatal cells + epidermal cells). Plant material was oven dried at 65°C for 4 d and weighed to determine total rosette dry weight.

Epidermal permeability was measured as described previously (Kosma et al., 2009). To quantify excised rosette water loss, 4-week-old plants were dark acclimated for 3 h prior to measurement. Whole rosettes were excised (from roots) and placed immediately in water in the dark and soaked for 60 min to equilibrate water contents. Rosettes removed from soaking were blotted dry to remove excess water, and weights were determined gravimetrically using a microbalance. Data were expressed as a percentage of the initial water-saturated fresh weight. Epidermal permeability was also assessed using chlorophyll efflux. Prior to measurement, 4-week-old plants were dark acclimated for 3 h, then rosettes were collected and immersed in equal volumes of 80% ethanol in glass scintillation vials, which were covered with aluminum foil and agitated gently on a shaker platform. Aliquots of 1 mL were removed every 20 min and 24 h after initial immersion. The amount of chlorophyll extracted into the solution was quantified and calculated from UV light absorption at 647 and 664 nm as described (Lolle et al., 1998). Data are expressed as percentages of the total chlorophyll extracted after 24 h in 80% ethanol.

For water soil deprivation experiments, plants were grown under optimal growth conditions as described previously (Joubès et al., 2008). Twenty-day-old plants were deprived of water until nearly all wild-type plants wilted (typically 20 d) and had reached a RWC of 48%. Control plants grown alongside water deficit-treated plants were watered as needed. For RWC measurements, rosette fresh weights were collected on a microbalance. Rosettes were then submerged in distilled, deionized water for 6 h, and blotted dry, and saturated fresh weights were determined. Rosettes were then dried in an oven at 80°C, and dry weights were determined. Rosette RWC was calculated as described by Barrs and Weatherley (1962).

For plant inoculations, leaves of 4-week-old plants were syringe infiltrated using *Pseudomonas syringae* pv *tomato DC3000* or *DC3000/avrRpt2* strains at the indicated bacterial densities. In planta bacterial growth and gene expression analyses were performed as described previously (Lorrain et al., 2004). For *Sclerotinia sclerotiorum* infection, leaves of 4-week-old plants were inoculated with *Sclerotinia* (strain S55) as described previously (Perchepied et al., 2010). Macroscopic observation of symptoms was performed, and disease symptoms were scored 7 d after inoculation with the mycelium. The Arabidopsis ecotypes Shahdara and Rubezhnoe-1 were used as susceptible and resistant controls, respectively.

DNA, RNA, and cDNA Preparation, Real-Time RT-PCR Conditions, and Analysis

Genomic DNA was extracted from Arabidopsis leaves with the DNeasy Plant kit (Qiagen), and RNA was extracted from Arabidopsis tissues with the RNeasy Plant mini kit (Qiagen). Purified RNA was treated with DNase I using the DNA-free kit (Ambion). First-strand cDNA was prepared from 1 μg of total RNA with the SuperScript RT II kit (Invitrogen) and oligo$(dT)_{18}$ according to the manufacturer's instructions. A 0.2-μL aliquot of the total reaction volume (20 μL) was used as a template in real time RT-mediated PCR amplification. The PCR amplification was performed with the gene-specific primers listed in Supplemental Table S1. PCR efficiency ranged from 95% to 105%. All samples were assayed in triplicate wells. Real-time PCR was performed on an iCycler (Bio-Rad). Samples were amplified in a 25-μL reaction containing 1× SYBR Green Master Mix (Bio-Rad) and 300 nM of each primer. The thermal profile consisted of one cycle at 95°C for 3 min and 30 s followed by 40 cycles at 95°C for 30 s and 58°C for 30 s. For each run, data acquisition and analysis were done using the iCycler iQ software (version 3.0a; Bio-Rad). The transcript abundance in samples was determined using a comparative threshold cycle method. The relative abundance of *ACT2*, *EF-1α*, *eIF-4A-1*, *UBQ10*, and *PP2A* mRNAs (Czechowski et al., 2005) in each sample was determined and used to normalize for differences of total RNA amount according to the method described by Vandesompele et al. (2002).

Cloning and Transgenic Plants

The *CER1* promoter sequence and the *CER1* open reading frame were amplified from Arabidopsis genomic DNA and from cDNA, respectively, using the primers listed in Supplemental Table S1. The corresponding PCR fragments were cloned into the pDONR207 ENTRY vector by the Gateway recombinational cloning technology and subsequently transferred into the pKGWFS7, pK7WG2D, and pH7WG2D Destination vectors (Karimi et al., 2002). Constructs transferred into the *Agrobacterium tumefaciens* C58C1Rif^R strain harboring the plasmid pMP90 were used to generate stably transformed Arabidopsis using the floral dip transformation method (Clough and Bent, 1998). Histochemical GUS analyses were performed as described (Joubès

et al., 2008). Quantitative fluorometric GUS assays were performed as described (Joubès et al., 2004).

Lipid Analyses

Cuticular Wax Analysis

Epicuticular waxes were extracted from leaves and stems by immersing tissues for 30 s in chloroform containing docosane as an internal standard. Extracts were dried under N_2 gas and derivatized by heating at 110°C for 15 min in *N*,*O*-bis(trimethylsilyl)trifluoroacetamide):trimethylchlorosilane (99:1; Sigma). Surplus *N*,*O*-bis(trimethylsilyl)trifluoroacetamide):trimethylchlorosilane was evaporated under N_2 gas, and samples were dissolved in hexane for analysis. Silylated samples were analyzed by gas chromatography with a Hewlett-Packard 5890 series II gas chromatograph equipped with a flame ionization detector and a 30-m, 0.32-mm HP-1 capillary column with helium as the carrier gas. The initial temperature of 50°C was held for 1 min, increased at 25°C min^{-1} to 150°C, held for 2 min at 150°C, increased again at 10°C min^{-1} to 320°C, and held for 16 min at 320°C. Injector and detector temperatures were set at 250°C. Quantification was based on flame ionization detector peak areas and the internal standard. The total amount of cuticular wax was expressed per unit of leaf or stem surface area. Areas were determined by ImageJ software (http://rsb.info.nih.gov/ij/) using digital images of leaves and stems. Molecular identities were determined using an Agilent 6850 gas chromatograph equipped with a 30-m, 0.25-mm HP-5MS column and an Agilent 5975 mass spectrometric detector (70 eV; mass-to-charge ratio of 50–750). The same gas chromatography program was used, with helium (1.5 mL min^{-1}) as the carrier gas. Segments from the apical part of the stem were mounted onto stubs, sputter coated with gold particles by a Polaron SC-500 (Emitech), and viewed with a FEI Quanta 200 microscope.

Analysis of Acyl-CoA Composition

Fresh young leaf and stem tissues from 5-week-old plants were collected and used for acyl-CoA extraction and profiling as described (Larson and Graham, 2001).

Analysis of Cutin Polyester Composition

Fresh leaf and stem tissues from 5-week-old plants were collected and immersed in hot isopropanol for 10 min at 80°C. After cooling, samples were extensively delipidated by extracting the soluble lipids, then dried and depolymerized as described (Domergue et al., 2010). Extraction, derivatization, and analysis were performed as described (Domergue et al., 2010).

Analysis of Total Fatty Acyl Chain Composition

Total fatty acyl chains from stems and leaves that had been first immersed for 45 s in chloroform to remove waxes were transesterified overnight and analyzed as described (Mongrand et al., 1997).

Sequence data from this article can be found in the Arabidopsis Genome Initiative or GenBank/EMBL databases under the following accession numbers: *CER1*, At1g02205; *CER1-like1*, At1g02190; *CER1-like2*, At2g37700; *CER1-like3*, At5g28280; *CER2*, At4g24510; *CER3*, At5g57800; *MAH1*, At1g57750; *Actin2*, At1g49240; *eIF4A-1*, At3g13920; *EF-1α*, At5g60390; *UBQ10*, At4g05320; *PP2A*, At1g13320.

Supplemental Data

The following materials are available in the online version of this article.

Supplemental Figure S1. Cuticular wax composition of inflorescence stems of Arabidopsis Col-0 (WT), *cer1-1*, *cer1-2*, *cer1-1R*, *CER1ox1*, and *CER1ox2* lines.

Supplemental Figure S2. Cuticular wax composition of rosette leaves of Arabidopsis Col-0 (WT), *cer1-1*, *cer1-2*, *cer1-1R*, *CER1ox1*, and *CER1ox2* lines.

Supplemental Figure S3. Acyl-CoA profiling of inflorescence stems and rosette leaves of Arabidopsis Col-0 (WT), *cer1-1*, and *CER1ox1* lines.

Supplemental Figure S4. Composition of residual bound lipids in inflorescence stems and rosette leaves of Arabidopsis Col-0 (WT), *cer1-1*, and *CER1ox1* lines.

Supplemental Figure S5. Total fatty acyl chain composition in inflorescence stems and rosette leaves of Arabidopsis Col-0 (WT), *cer1-1*, and *CER1ox1* lines.

Supplemental Table S1. Primers used for PCR cloning and quantitative PCR analysis.

ACKNOWLEDGMENTS

We thank the Salk Institute for Genomic Analysis Laboratory and the Arabidopsis Biological Resource Center for providing the sequence-indexed Arabidopsis T-DNA insertion lines. We thank Owen Rowland (Carleton University) for providing seeds. We thank Isabelle Svahn from the Bordeaux Imaging Center (University Bordeaux Segalen) for help with scanning electron microscopy analysis. We thank Dr. V. Coulon for help in preparing the manuscript.

Received February 11, 2011; accepted March 7, 2011; published March 8, 2011.

LITERATURE CITED

Aarts MG, Keijzer CJ, Stiekema WJ, Pereira A (1995) Molecular characterization of the *CER1* gene of *Arabidopsis* involved in epicuticular wax biosynthesis and pollen fertility. Plant Cell **7:** 2115–2127

Aguirrezabal L, Bouchier-Combaud S, Radziejwoski A, Dauzat M, Cookson SJ, Granier C (2006) Plasticity to soil water deficit in Arabidopsis thaliana: dissection of leaf development into underlying growth dynamic and cellular variables reveals invisible phenotypes. Plant Cell Environ **29:** 2216–2227

Aharoni A, Dixit S, Jetter R, Thoenes E, van Arkel G, Pereira A (2004) The SHINE clade of AP2 domain transcription factors activates wax biosynthesis, alters cuticle properties, and confers drought tolerance when overexpressed in *Arabidopsis*. Plant Cell **16:** 2463–2480

Ariizumi T, Hatakeyama K, Hinata K, Sato S, Kato T, Tabata S, Toriyama K (2003) A novel male-sterile mutant of *Arabidopsis thaliana*, *faceless pollen-1*, produces pollen with a smooth surface and an acetolysis-sensitive exine. Plant Mol Biol **53:** 107–116

Bach L, Michaelson LV, Haslam R, Bellec Y, Gissot L, Marion J, Da Costa M, Boutin JP, Miquel M, Tellier F, et al (2008) The very-long-chain hydroxy fatty acyl-CoA dehydratase PASTICCINO2 is essential and limiting for plant development. Proc Natl Acad Sci USA **105:** 14727–14731

Barrs HD, Weatherley PE (1962) A re-examination of the relative turgidity technique for estimating water deficits in leaves. Aust J Biol Sci **15:** 413–428

Beaudoin F, Wu X, Li F, Haslam RP, Markham JE, Zheng H, Napier JA, Kunst L (2009) Functional characterization of the Arabidopsis beta-ketoacyl-coenzyme A reductase candidates of the fatty acid elongase. Plant Physiol **150:** 1174–1191

Bessire M, Chassot C, Jacquat AC, Humphry M, Borel S, Petétot JM, Métraux JP, Nawrath C (2007) A permeable cuticle in *Arabidopsis* leads to a strong resistance to *Botrytis cinerea*. EMBO J **26:** 2158–2168

Cameron KD, Teece MA, Smart LB (2006) Increased accumulation of cuticular wax and expression of lipid transfer protein in response to periodic drying events in leaves of tree tobacco. Plant Physiol **140:** 176–183

Chassot C, Nawrath C, Métraux JP (2007) Cuticular defects lead to full immunity to a major plant pathogen. Plant J **49:** 972–980

Chassot C, Nawrath C, Métraux JP (2008) The cuticle: not only a barrier for plant defence. A novel defence syndrome in plants with cuticular defects. Plant Signal Behav **3:** 142–144

Cheesbrough TM, Kolattukudy PE (1984) Alkane biosynthesis by decarbonylation of aldehydes catalyzed by a particulate preparation from *Pisum sativum*. Proc Natl Acad Sci USA **81:** 6613–6617

Chen X, Goodwin SM, Boroff VL, Liu X, Jenks MA (2003) Cloning and characterization of the *WAX2* gene of *Arabidopsis* involved in cuticle membrane and wax production. Plant Cell **15:** 1170–1185

Clough SJ, Bent AF (1998) Floral dip: a simplified method for Agrobacterium-mediated transformation of *Arabidopsis thaliana*. Plant J **16:** 735–743

Curvers K, Seifi H, Mouille G, de Rycke R, Asselbergh B, Van Hecke A, Vanderschaeghe D, Höfte H, Callewaert N, Van Breusegem F, et al (2010) Abscisic acid deficiency causes changes in cuticle permeability and pectin composition that influence tomato resistance to *Botrytis cinerea*. Plant Physiol **154:** 847–860

Czechowski T, Stitt M, Altmann T, Udvardi MK, Scheible WR (2005) Genome-wide identification and testing of superior reference genes for transcript normalization in Arabidopsis. Plant Physiol **139:** 5–17

Debono A, Yeats TH, Rose JK, Bird D, Jetter R, Kunst L, Samuels L (2009) *Arabidopsis* LTPG is a glycosylphosphatidylinositol-anchored lipid transfer protein required for export of lipids to the plant surface. Plant Cell **21:** 1230–1238

Denic V, Weissman JS (2007) A molecular caliper mechanism for determining very long-chain fatty acid length. Cell **130:** 663–677

Dennis M, Kolattukudy PE (1992) A cobalt-porphyrin enzyme converts a fatty aldehyde to a hydrocarbon and CO. Proc Natl Acad Sci USA **89:** 5306–5310

Domergue F, Vishwanath SJ, Joubès J, Ono J, Lee JA, Bourdon M, Alhattab R, Lowe C, Pascal S, Lessire R, et al (2010) Three Arabidopsis fatty acyl-coenzyme A reductases, FAR1, FAR4, and FAR5, generate primary fatty alcohols associated with suberin deposition. Plant Physiol **153:** 1539–1554

Duan H, Schuler MA (2005) Differential expression and evolution of the Arabidopsis *CYP86A* subfamily. Plant Physiol **137:** 1067–1081

Efremova N, Schreiber L, Bär S, Heidmann I, Huijser P, Wellesen K, Schwarz-Sommer Z, Saedler H, Yephremov A (2004) Functional conservation and maintenance of expression pattern of *FIDDLEHEAD-like* genes in *Arabidopsis* and *Antirrhinum*. Plant Mol Biol **56:** 821–837

Eigenbrode SD, Rayor L, Chow J, Latty P (2000) Effects of wax bloom variation in *Brassica oleracea* on foraging by a vespid wasp. Entomol Exp Appl **97:** 161–166

Feng L, Zhang Y, Xi J, Zhu Y, Wang N, Xia F, Jiang L (2008) Petal effect: a superhydrophobic state with high adhesive force. Langmuir **24:** 4114–4119

Granier C, Aguirrezabal L, Chenu K, Cookson SJ, Dauzat M, Hamard P, Thioux JJ, Rolland G, Bouchier-Combaud S, Lebaudy A, et al (2006) PHENOPSIS, an automated platform for reproducible phenotyping of plant responses to soil water deficit in *Arabidopsis thaliana* permitted the identification of an accession with low sensitivity to soil water deficit. New Phytol **169:** 623–635

Greer S, Wen M, Bird D, Wu X, Samuels L, Kunst L, Jetter R (2007) The cytochrome P450 enzyme CYP96A15 is the midchain alkane hydroxylase responsible for formation of secondary alcohols and ketones in stem cuticular wax of Arabidopsis. Plant Physiol **145:** 653–667

Hannoufa A, McNevin J, Lemieux B (1993) Epicuticular waxes of *eceriferum* mutants of *Arabidopsis thaliana*. Phytochemistry **33:** 851–855

Hegde Y, Kolattukudy PE (1997) Cuticular waxes relieve self-inhibition of germination and appressorium formation by the conidia of *Magnaporthe grisea*. Physiol Plant Pathol **51:** 75–84

Hooker TS, Millar AA, Kunst L (2002) Significance of the expression of the CER6 condensing enzyme for cuticular wax production in Arabidopsis. Plant Physiol **129:** 1568–1580

Hülskamp M, Kopczak SD, Horejsi TF, Kihl BK, Pruitt RE (1995) Identification of genes required for pollen-stigma recognition in *Arabidopsis thaliana*. Plant J **8:** 703–714

Jenks MA, Andersen L, Teusink RS, Williams MH (2001) Leaf cuticular waxes of potted rose cultivars as affected by plant development, drought and paclobutrazol treatments. Physiol Plant **112:** 62–70

Jenks MA, Tuttle HA, Eigenbrode SD, Feldmann KA (1995) Leaf epicuticular waxes of the *eceriferum* mutants in Arabidopsis. Plant Physiol **108:** 369–377

Jetter R, Kunst L (2008) Plant surface lipid biosynthetic pathways and their utility for metabolic engineering of waxes and hydrocarbon biofuels. Plant J **54:** 670–683

Joubès J, De Schutter K, Verkest A, Inzé D, De Veylder L (2004) Conditional, recombinase-mediated expression of genes in plant cell cultures. Plant J **37:** 889–896

Joubès J, Raffaele S, Bourdenx B, Garcia C, Laroche-Traineau J, Moreau P, Domergue F, Lessire R (2008) The VLCFA elongase gene family in *Arabidopsis thaliana*: phylogenetic analysis, 3D modelling and expression profiling. Plant Mol Biol **67:** 547–566

Kamigaki A, Kondo M, Mano S, Hayashi M, Nishimura M (2009) Suppression of peroxisome biogenesis factor 10 reduces cuticular wax accumulation by disrupting the ER network in Arabidopsis thaliana. Plant Cell Physiol **50:** 2034–2046

Karimi M, Inzé D, Depicker A (2002) GATEWAY vectors for *Agrobacterium*-mediated plant transformation. Trends Plant Sci **7:** 193–195

Kerstiens G (1996) Cuticular water permeability and its physiologial significance. J Exp Bot **47:** 1813–1832

Koch K, Neinhuis C, Ensikat HJ, Barthlott W (2004) Self assembly of epicuticular waxes on living plant surfaces imaged by atomic force microscopy (AFM). J Exp Bot **55:** 711–718

Koornneef M, Hanhart CJ, Thiel F (1989) A genetic and phenotypic description of *Eceriferum* (*cer*) mutants in *Arabidopsis thaliana*. J Hered **80:** 118–122

Kosma DK, Bourdenx B, Bernard A, Parsons EP, Lü S, Joubès J, Jenks MA (2009) The impact of water deficiency on leaf cuticle lipids of Arabidopsis. Plant Physiol **151:** 1918–1929

Kosma DK, Jenks MA (2007). Eco-physiological and molecular-genetic determinants of plant cuticle function in drought and salt stress tolerance. *In* MA Jenks, PM Hasegawa, SM Jain, eds, Advances in Molecular Breeding toward Drought and Salt Tolerant Crops. Springer, Dordrecht, The Netherlands, 91–120

Kunst L, Clemens S, Hooker T (2000) Expression of the wax-specific condensing enzyme CUT1 in *Arabidopsis*. Biochem Soc Trans **28:** 651–654

Kunst L, Samuels AL (2003) Biosynthesis and secretion of plant cuticular wax. Prog Lipid Res **42:** 51–80

Kunst L, Samuels L (2009) Plant cuticles shine: advances in wax biosynthesis and export. Curr Opin Plant Biol **12:** 721–727

Kurata T, Kawabata-Awai C, Sakuradani E, Shimizu S, Okada K, Wada T (2003) The *YORE-YORE* gene regulates multiple aspects of epidermal cell differentiation in *Arabidopsis*. Plant J **36:** 55–66

Kurdyukov S, Faust A, Nawrath C, Bär S, Voisin D, Efremova N, Franke R, Schreiber L, Saedler H, Métraux JP, et al (2006a) The epidermis-specific extracellular *BODYGUARD* controls cuticle development and morphogenesis in *Arabidopsis*. Plant Cell **18:** 321–339

Kurdyukov S, Faust A, Trenkamp S, Bär S, Franke R, Efremova N, Tietjen K, Schreiber L, Saedler H, Yephremov A (2006b) Genetic and biochemical evidence for involvement of *HOTHEAD* in the biosynthesis of long-chain alpha-,omega-dicarboxylic fatty acids and formation of extracellular matrix. Planta **224:** 315–329

Larson TR, Graham IA (2001) Technical Advance. A novel technique for the sensitive quantification of acyl CoA esters from plant tissues. Plant J **25:** 115–125

Li F, Wu X, Lam P, Bird D, Zheng H, Samuels L, Jetter R, Kunst L (2008) Identification of the wax ester synthase/acyl-coenzyme A:diacylglycerol acyltransferase WSD1 required for stem wax ester biosynthesis in Arabidopsis. Plant Physiol **148:** 97–107

Li Y, Beisson F (2009) The biosynthesis of cutin and suberin as an alternative source of enzymes for the production of bio-based chemicals and materials. Biochimie **91:** 685–691

Li Y, Beisson F, Koo AJ, Molina I, Pollard M, Ohlrogge J (2007) Identification of acyltransferases required for cutin biosynthesis and production of cutin with suberin-like monomers. Proc Natl Acad Sci USA **104:** 18339–18344

Lolle SJ, Hsu W, Pruitt RE (1998) Genetic analysis of organ fusion in Arabidopsis thaliana. Genetics **149:** 607–619

Lorrain S, Lin B, Auriac MC, Kroj T, Saindrenan P, Nicole M, Balagué C, Roby D (2004) Vascular associated death1, a novel GRAM domain-containing protein, is a regulator of cell death and defense responses in vascular tissues. Plant Cell **16:** 2217–2232

Lü S, Song T, Kosma DK, Parsons EP, Rowland O, Jenks MA (2009) *Arabidopsis CER8* encodes LONG-CHAIN ACYL-COA SYNTHETASE 1 (LACS1) that has overlapping functions with LACS2 in plant wax and cutin synthesis. Plant J **59:** 553–564

Markham JE, Jaworski JG (2007) Rapid measurement of sphingolipids from *Arabidopsis thaliana* by reversed-phase high-performance liquid chromatography coupled to electrospray ionization tandem mass spectrometry. Rapid Commun Mass Spectrom **21:** 1304–1314

Massonnet C, Vile D, Fabre J, Hannah MA, Caldana C, Lisec J, Beemster GT, Meyer RC, Messerli G, Gronlund JT, et al (2010) Probing the reproducibility of leaf growth and molecular phenotypes: a comparison

of three Arabidopsis accessions cultivated in ten laboratories. Plant Physiol **152:** 2142–2157

Mayfield JA, Preuss D (2000) Rapid initiation of *Arabidopsis* pollination requires the oleosin-domain protein GRP17. Nat Cell Biol **2:** 128–130

McNevin JP, Woodward W, Hannoufa A, Feldmann KA, Lemieux B (1993) Isolation and characterization of *eceriferum* (*cer*) mutants induced by T-DNA insertions in *Arabidopsis thaliana*. Genome **36:** 610–618

Mongrand S, Bessoule JJ, Cassagne C (1997) A re-examination in vivo of the phosphatidylcholine-galactolipid metabolic relationship during plant lipid biosynthesis. Biochem J (Pt 3) **327:** 853–858

Panikashvili D, Savaldi-Goldstein S, Mandel T, Yifhar T, Franke RB, Höfer R, Schreiber L, Chory J, Aharoni A (2007) The Arabidopsis DESPERADO/AtWBC11 transporter is required for cutin and wax secretion. Plant Physiol **145:** 1345–1360

Perchepied L, Balagué C, Riou C, Claudel-Renard C, Rivière N, Grezes-Besset B, Roby D (2010) Nitric oxide participates in the complex interplay of defense-related signaling pathways controlling disease resistance to *Sclerotinia sclerotiorum* in *Arabidopsis thaliana*. Mol Plant Microbe Interact **23:** 846–860

Pighin JA, Zheng H, Balakshin LJ, Goodman IP, Western TL, Jetter R, Kunst L, Samuels AL (2004) Plant cuticular lipid export requires an ABC transporter. Science **306:** 702–704

Podila GK, Rogers LM, Kolattukudy PE (1993) Chemical signals from avocado surface wax trigger germination and appressorium formation in *Colletotrichum gloeosporioides*. Plant Physiol **103:** 267–272

Pollard M, Beisson F, Li Y, Ohlrogge JB (2008) Building lipid barriers: biosynthesis of cutin and suberin. Trends Plant Sci **13:** 236–246

Preuss D, Lemieux B, Yen G, Davis RW (1993) A conditional sterile mutation eliminates surface components from *Arabidopsis* pollen and disrupts cell signaling during fertilization. Genes Dev **7:** 974–985

Raffaele S, Leger A, Roby D (2009) Very long chain fatty acid and lipid signaling in the response of plants to pathogens. Plant Signal Behav **4:** 94–99

Raffaele S, Vailleau F, Léger A, Joubès J, Miersch O, Huard C, Blée E, Mongrand S, Domergue F, Roby D (2008) A MYB transcription factor regulates very-long-chain fatty acid biosynthesis for activation of the hypersensitive cell death response in *Arabidopsis*. Plant Cell **20:** 752–767

Reina-Pinto JJ, Yephremov A (2009) Surface lipids and plant defenses. Plant Physiol Biochem **47:** 540–549

Reisige K, Gorzelanny C, Daniels U, Moerschbacher BM (2006) The C28 aldehyde octacosanal is a morphogenetically active component involved in host plant recognition and infection structure differentiation in the wheat stem rust fungus. Physiol Mol Plant Pathol **68:** 33–40

Riederer M (2006) Thermodynamics of the water permeability of plant cuticles: characterization of the polar pathway. J Exp Bot **57:** 2937–2942

Rowland O, Lee R, Franke R, Schreiber L, Kunst L (2007) The *CER3* wax biosynthetic gene from *Arabidopsis thaliana* is allelic to *WAX2/YRE/FLP1*. FEBS Lett **581:** 3538–3544

Rowland O, Zheng H, Hepworth SR, Lam P, Jetter R, Kunst L (2006) *CER4* encodes an alcohol-forming fatty acyl-coenzyme A reductase involved in cuticular wax production in Arabidopsis. Plant Physiol **142:** 866–877

Samuels L, Kunst L, Jetter R (2008) Sealing plant surfaces: cuticular wax formation by epidermal cells. Annu Rev Plant Biol **59:** 683–707

Schneider-Belhaddad F, Kolattukudy P (2000) Solubilization, partial purification, and characterization of a fatty aldehyde decarbonylase from a higher plant, *Pisum sativum*. Arch Biochem Biophys **377:** 341–349

Schnurr J, Shockey J, Browse J (2004) The acyl-CoA synthetase encoded by *LACS2* is essential for normal cuticle development in *Arabidopsis*. Plant Cell **16:** 629–642

Shepherd T, Wynne Griffiths D (2006) The effects of stress on plant cuticular waxes. New Phytol **171:** 469–499

Suh MC, Samuels AL, Jetter R, Kunst L, Pollard M, Ohlrogge J, Beisson F (2005) Cuticular lipid composition, surface structure, and gene expression in Arabidopsis stem epidermis. Plant Physiol **139:** 1649–1665

Tang D, Simonich MT, Innes RW (2007) Mutations in LACS2, a long-chain acyl-coenzyme A synthetase, enhance susceptibility to avirulent *Pseudomonas syringae* but confer resistance to *Botrytis cinerea* in Arabidopsis. Plant Physiol **144:** 1093–1103

Tisné S, Schmalenbach I, Reymond M, Dauzat M, Pervent M, Vile D, Granier C (2010). Keep on growing under drought: genetic and developmental bases of the response of rosette area using a recombinant inbred line population. Plant Cell Environ **33:** 1875–1887

Vandesompele J, De Preter K, Pattyn F, Poppe B, Van Roy N, De Paepe A, Speleman F (2002) Accurate normalization of real-time quantitative RT-PCR data by geometric averaging of multiple internal control genes. Genome Biol **3:** H0034

Wellesen K, Durst F, Pinot F, Benveniste I, Nettesheim K, Wisman E, Steiner-Lange S, Saedler H, Yephremov A (2001) Functional analysis of the *LACERATA* gene of *Arabidopsis* provides evidence for different roles of fatty acid omega-hydroxylation in development. Proc Natl Acad Sci USA **98:** 9694–9699

Weng H, Molina I, Shockey J, Browse J (2010) Organ fusion and defective cuticle function in a *lacs1 lacs2* double mutant of *Arabidopsis*. Planta **231:** 1089–1100

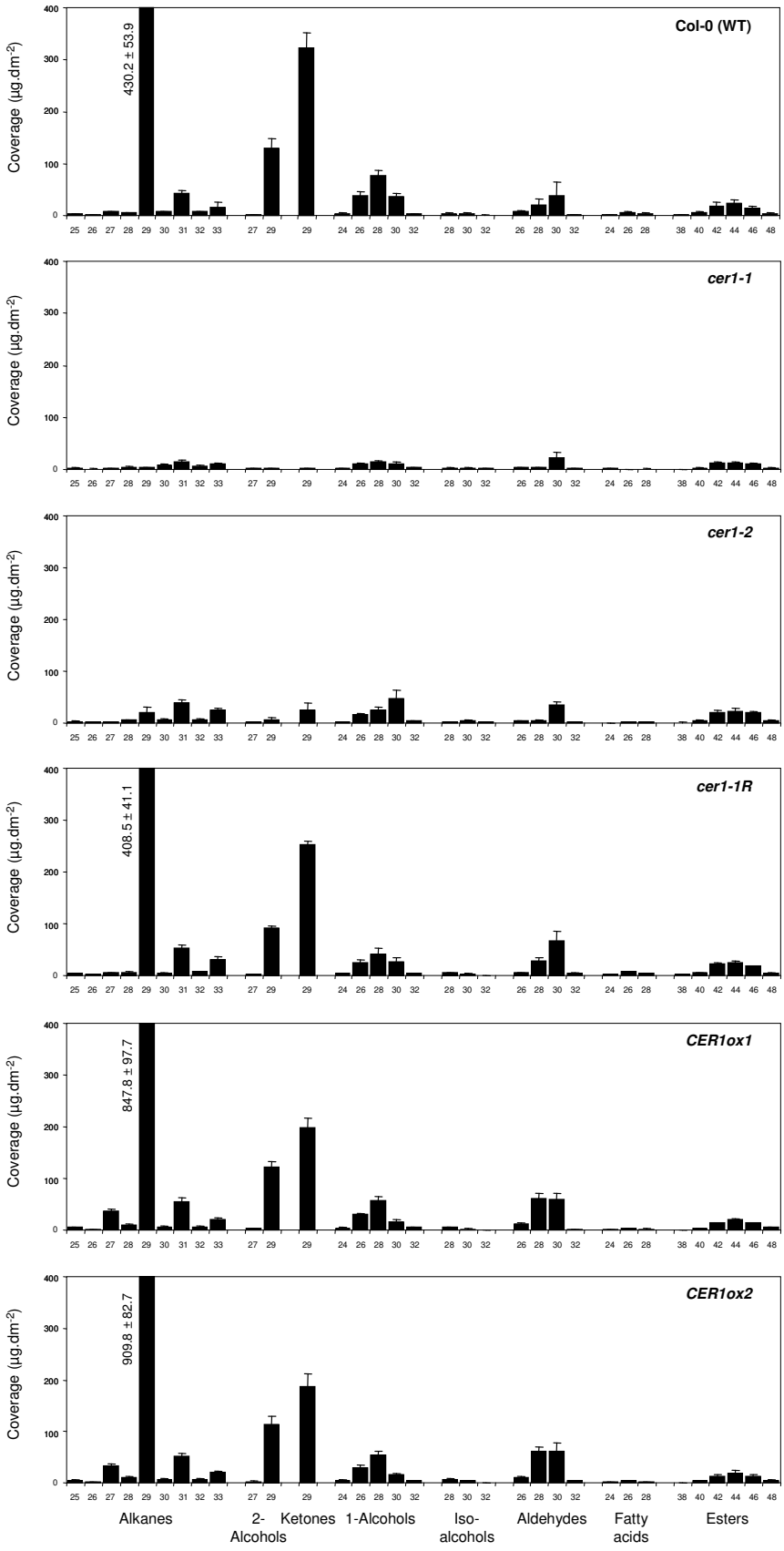
Xiao F, Goodwin SM, Xiao Y, Sun Z, Baker D, Tang X, Jenks MA, Zhou JM (2004) *Arabidopsis* CYP86A2 represses *Pseudomonas syringae* type III genes and is required for cuticle development. EMBO J **23:** 2903–2913

Yang M, Yang Q, Fu T, Zhou Y (2011) Overexpression of the Brassica napus BnLAS gene in Arabidopsis affects plant development and increases drought tolerance. Plant Cell Rep **30:** 373–388

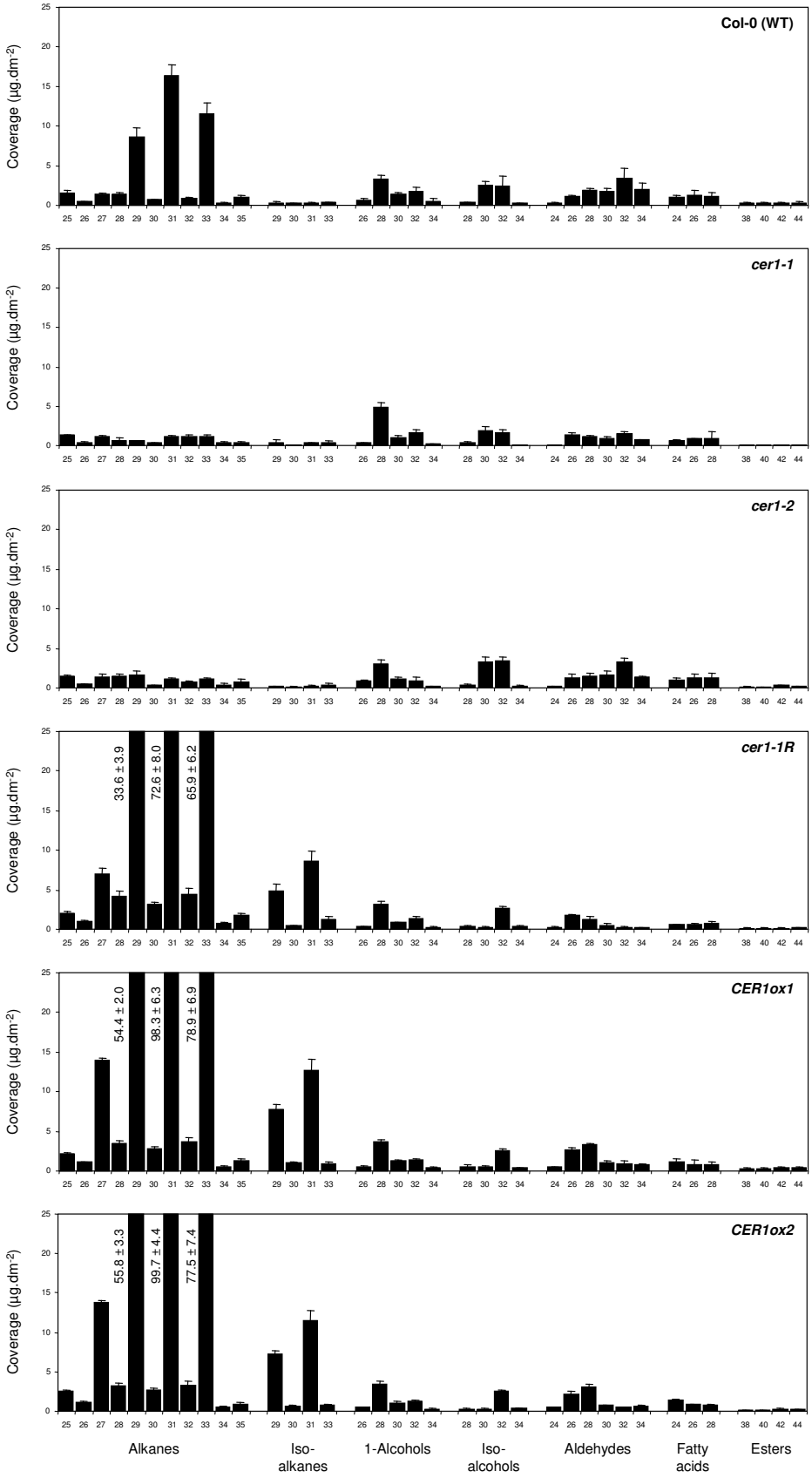
Zhang JY, Broeckling CD, Blancaflor EB, Sledge MK, Sumner LW, Wang ZY (2005) Overexpression of WXP1, a putative *Medicago truncatula* AP2 domain-containing transcription factor gene, increases cuticular wax accumulation and enhances drought tolerance in transgenic alfalfa (Medicago sativa). Plant J **42:** 689–707

Zhang JY, Broeckling CD, Sumner LW, Wang ZY (2007) Heterologous expression of two *Medicago truncatula* putative ERF transcription factor genes, WXP1 and WXP2, in *Arabidopsis* led to increased leaf wax accumulation and improved drought tolerance, but differential response in freezing tolerance. Plant Mol Biol **64:** 265–278

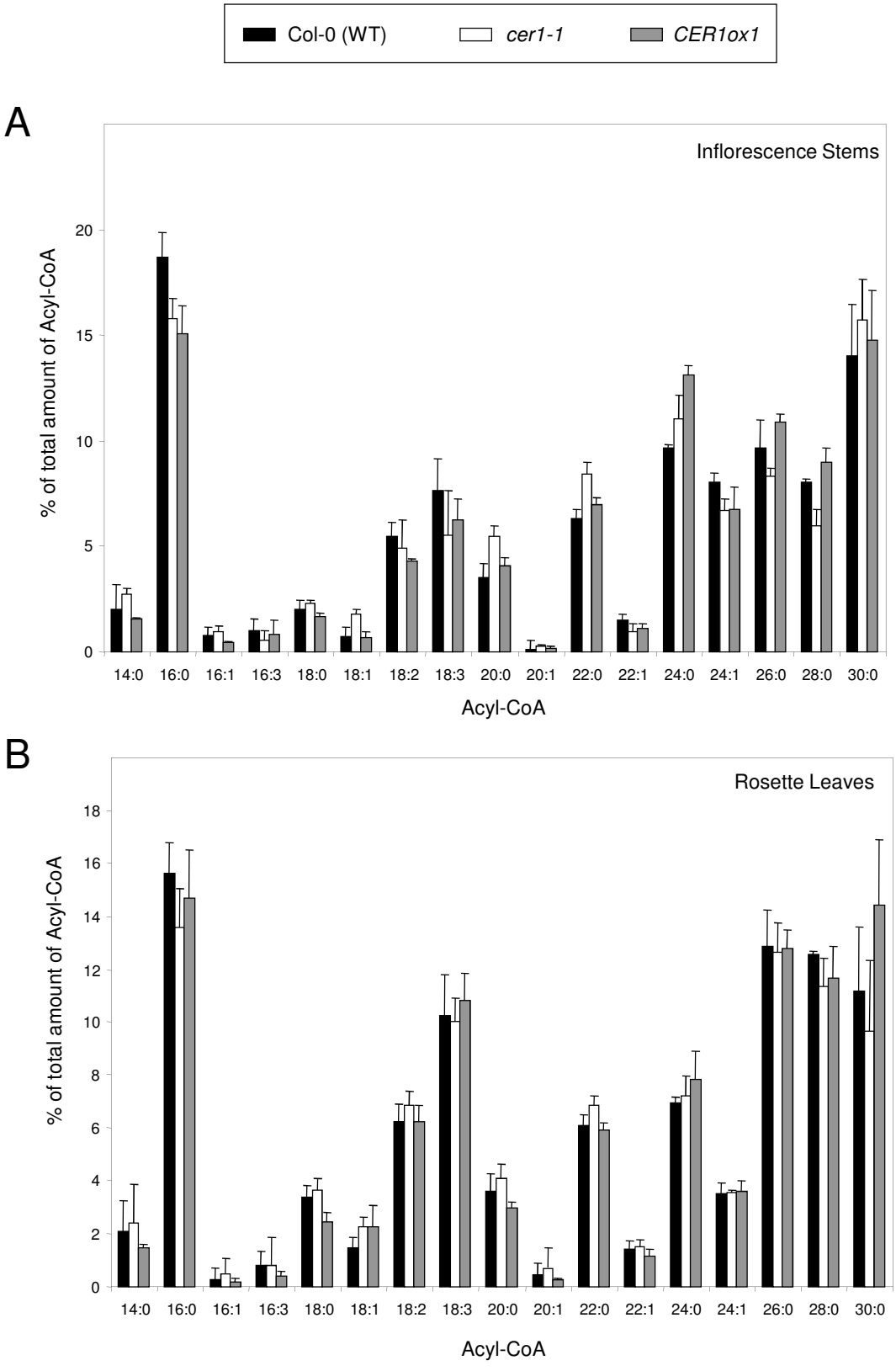
Zheng H, Rowland O, Kunst L (2005) Disruptions of the *Arabidopsis* enoyl-CoA reductase gene reveal an essential role for very-long-chain fatty acid synthesis in cell expansion during plant morphogenesis. Plant Cell **17:** 1467–1481



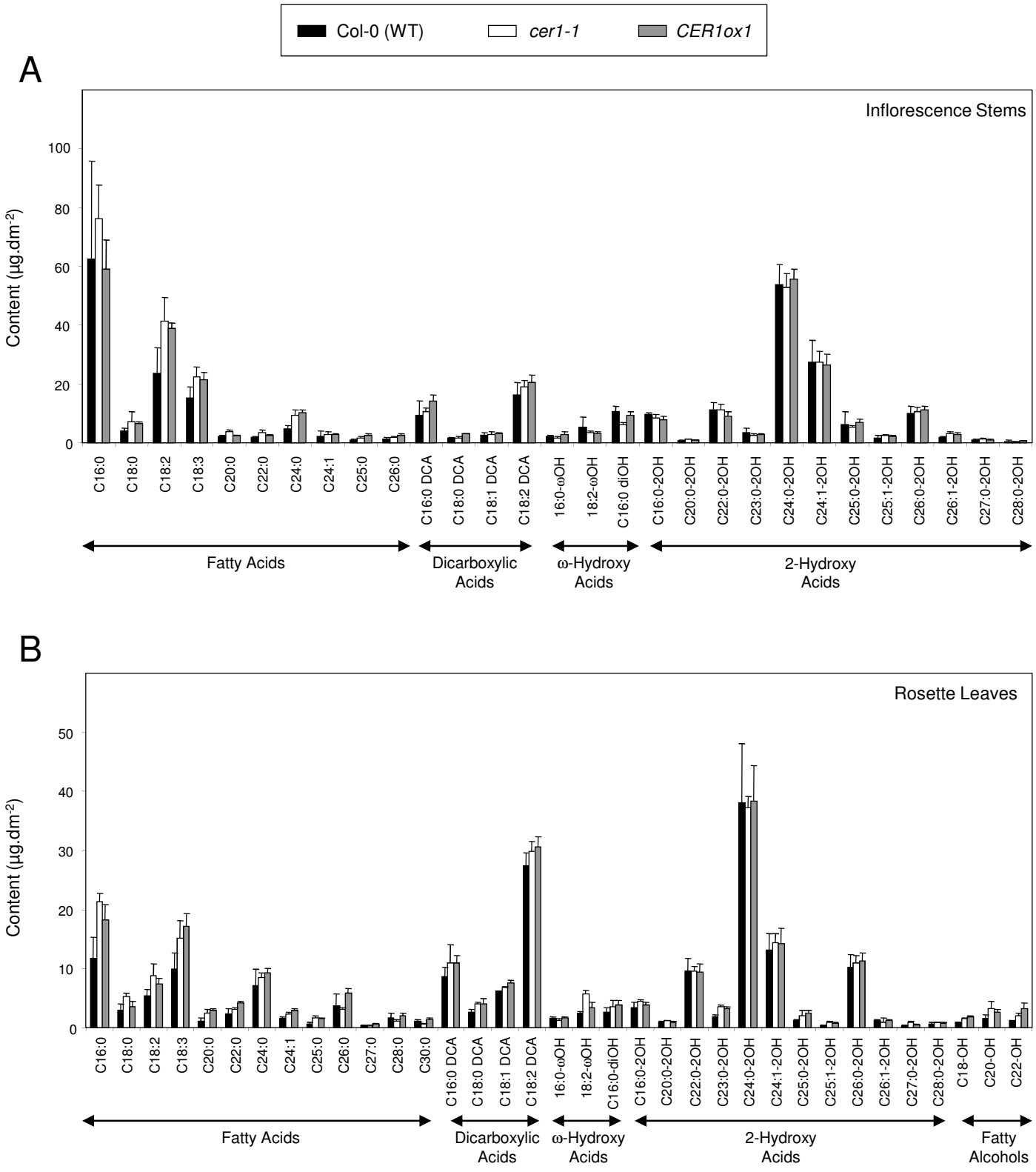
Supplemental Figure S1. Cuticular wax composition of inflorescence stems of Arabidopsis Col-0 (WT), *cer1-1*, *cer1-2*, *cer1-1R*, *CER1ox1* and *CER1ox2* lines. Wax coverage is expressed as µg.dm^{-2} of stem surface area. Each wax constituent is designated by carbon chain-length and is labelled by chemical class along the x-axis. Each value represents the mean ±S.D. of four replicates.



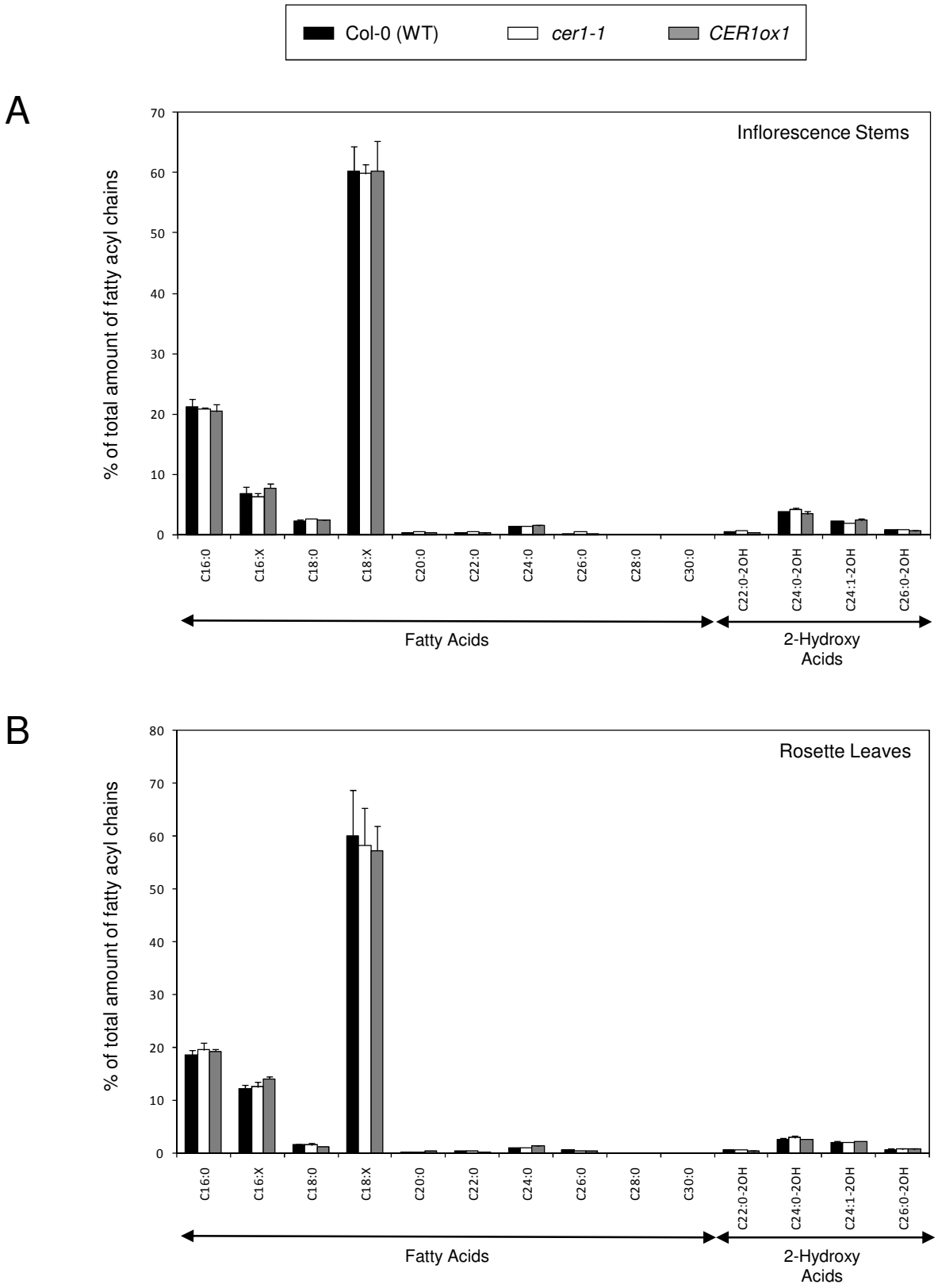
Supplemental Figure S2. Cuticular wax composition of rosette leaves of Arabidopsis Col-0 (WT), *cer1-1*, *cer1-2*, *cer1-1R*, *CER1ox1* and *CER1ox2* lines. Wax coverage is expressed as µg.dm^{-2} of leaf surface area. Each wax constituent is designated by carbon chain-length and is labelled by chemical class along the x-axis. Each value represents the mean ±S.D. of four replicates.



Supplemental Figure S3. Acyl-CoA profiling of inflorescence stems (A) and rosette leaves (B) of Arabidopsis Col-0 (WT), *cer1-1*, and *CER1ox1* lines. Each constituent is designated by carbon chain-length along the x-axis. Each value represents the mean ±S.D. of four replicates.



Supplemental Figure S4. Composition of residual bound lipids in inflorescence stems (A) and rosette leaves (B) of Arabidopsis Col-0 (WT), *cer1-1*, and *CER1ox1* lines. Each constituent is designated by carbon chain-length and labelled by chemical class along the x-axis. Each value represents the mean ± S.D. of three to four replicates.



Supplemental Figure S5. Total fatty acyl chain composition in inflorescence stems (A) and rosette leaves (B) of Arabidopsis Col-0 (WT), *cer1-1*, and *CER1ox1* lines. Each constituent is designated by carbon chain-length and labelled by chemical class along the x-axis. Each value represents the mean ± S.D. of three to four replicates.

Supplemental Table S1: Primers used for PCR cloning and QPCR analysis

Gene	Arabidopsis Genome Initiative ID	Forward Primer (5′ 3′)	Reverse Primer (5′ 3′)
Primers used for QPCR analysis			
ACT2	At1g49240	CCGAGCAGCATGAAGATTAAG	CATACTCTGCCTTAGAGATCCACA
eIF4A-1	At3g13920	CTGATTTTGACCCGTCGTCT	AAGACAAACAACAAAGCCGAAT
EF-1a	At5g60390	TCGTTATGATCGACTCTCTTATGG	CCAAAAAGGAGGGAGAGAGAAAG
UBQ10	At4g05320	GGCCTTGTATAATCCCTGATGAATAAG	AAAGAGATAACAGGAACGGAAACATAGT
PP2A	At1g13320	TAACGTGGCCAAAATGATGC	GTTCTCCACAACCGCTTGGT
CER1	AT1G02205	AAGGATGGGAAATGCATGAG	TGATGTGGAAGGAGGAGAGG
CER1 like1	At1g02190	GCCATGATTTCCAACCTCTC	CAGCAAACAATGATGGAAGG
CER1 like2	At2g37700	GGTGAAGAATTAAATGGGTATGGA	TGCTATGAAGCACCACCTCA
CER1 like3	At5g28280	AGCTCGTTTGTTCGTGGATT	TCAAAGGCTAGACAAATGATCG
CER3	At5g57800	AAAGGAGATGCAAGCAGGAA	TTTTCTTGGAAATTAGGTGCAT
CYP96A15	At1g57750	GCTTGGCTTCTACGGCAACT	TATGAGCATGACGTGGGACA
RD29A	At5g52310	TGTCGACGAGAAGCAAAGAA	CGGGAAAACAACTCCTGATT
Primers used for cloning of promoter sequences			
CER1	AT1G02205	AAAAGCAGGCTAGAAACAGTGCTATGATC	AGAAAGCTGGGTTATACCGTCGAATGTAA
Primers used for cloning of full length cDNA			
CER1	AT1G02205	AAAAGCAGGCTTAATGGCCACAAAACCAGGA	AGAAAGCTGGGTCTAATAAATTAGTTGGAT